Chapter 2

Large scale Variations in Gain

2.1 INTRODUCTION

In this chapter we will study the large scale variations in the channel that are captured in the power gain term $G(d, \vartheta)$ of (1.16). The variation of $G(d, \vartheta)$ with location is in general quite complex and nature of the variation changes from one geographical region to the next. Measurements of $G(d, \vartheta)$ can be obtained through drive tests or through detailed simulation using all the characteristics of the environment, after averaging out the small scale variations. While the details of $G(d, \vartheta)$ may be useful for certain kinds of cellular planning to avoid "holes" in coverage, no such detailed model can ever be accurate since the environment could change. More importantly, these details will be too cumbersome to be useful in design and analysis of wireless communication systems.

We will hence try and capture the essential features of $G(d, \vartheta)$ in a useful parametric model with a few parameters. As we shall see, this process is facilitated by resorting to a stochastic model for $G(d, \vartheta)$. In cellular systems, for example, some of these parameters can be expected to remain constant over regions of the cell, and they can be estimated from field trials or simulations and stored at the basestation. Other parameters can be estimated online based on measurements taken on a pilot signal broadcast by the basestation.

2.2 MEDIAN COMPONENT OF GAIN

To understand the variations in $G(d, \vartheta)$ with location, we appeal to the physics of electromagnetic wave propagation. For radiation in free space, Friis equation [Par98] dictates that the received power should decay with distance from the transmitter as d^{-2} (note that there is no dependence on ϑ). However in a realistic propagation environment, there are several scatterers that reflect the wave, and also possibly refract or defract the wave before it reaches the receiver. Thus the power gain $G(d, \vartheta)$ has a much more complicated variation with location. The book by Parsons [Par98] gives an excellent introduction to the various modes of propagation in a typical wireless environment, and their effect on the power gain. However, as noted earlier, a detailed study of the propagation physics is futile since the resulting description of $G(d, \vartheta)$ would be too cumbersome to be useful. Nevertheless, we use the intuition from physics to argue that $G(d, \vartheta)$ should have a "mean" variation

that is monotonically decreasing in d and is independent of ϑ. This motivates the following model for $G(d, \vartheta)$:

$$G(d, \vartheta) = S(d, \vartheta)\bar{G}(d) \, . \tag{2.1}$$

where $\bar{G}(d)$ is the monotonic component. Note that we can always write G in this fashion if we allow S and $\bar{G}$ to be arbitrary. Our goal is to find the $\bar{G}$ that "best" fits the variation in G. In order to do this, it is more convenient to rewrite the above equation in dB as

$$G(d, \vartheta)[\text{dB}] = Z(d, \vartheta) + \bar{G}(d)[\text{dB}] \, , \tag{2.2}$$

where $Z(d, \vartheta) = 10 \log S(d, \vartheta)$. Now $\bar{G}(d)[\text{dB}]$ can indeed be considered as the mean variation of $G(d, \vartheta)[\text{dB}]$, with $Z(d, \vartheta)$ being the variation around the mean. The problem of finding the best $\bar{G}(d)[\text{dB}]$ is facilitated by using a parametric model. This is where we resort to propagation physics to argue that $\bar{G}(d)$ should be roughly of the form ad^{-b}, where $b > 0$, i.e., that $\bar{G}(d)[\text{dB}]$ is of the form

$$\bar{G}(d)[\text{dB}] \sim A - B \log d \, . \tag{2.3}$$

More generally, we could model $\bar{G}(d)[\text{dB}]$ as being piece-wise linear in $\log d$. The simple linear model is quite accurate for outdoor channels, whereas a piece-wise linear model may be more appropriate for indoor channels [Stu96, Pg. 104]. There is also experimental evidence [**?**] that suggests that $\bar{G}(d)$ falls off exponentially for large values of d, i.e., that $\bar{G}(d)[\text{dB}]$ is eventually linear in d. Recent work by Franceschetti et al [**?**] based on a wandering photon model provides a theoretical justification for this exponential tail.

To obtain the constants A and B for a given region we use linear regression on measured values of $G(d, \vartheta)[\text{dB}]$ obtained via drive tests or via detailed simulation. Then, A and B will correspond to the best "cone" fit to $G(d, \vartheta)[\text{dB}]$ and $Z(d, \vartheta)$ will represent the error (see Fig. 2.1). There have been attempts to generate generic rough estimates of A and B for various kinds of environments using extensive measurements (see, e.g., the models of Okumura and Hata in [Stu96, Pg. 95]). Clearly, the most accurate computation of $\bar{G}(d)$ is obtained from drive tests taken in the cell. Also, the more accurate the curve fit for the mean, the smaller the variance of the error term $Z(d, \vartheta)$. Of course, no matter how accurate we make our model for $\bar{G}(d)$, variance of $Z(d, \vartheta)$ cannot be made zero, since G is a function of both d and ϑ.

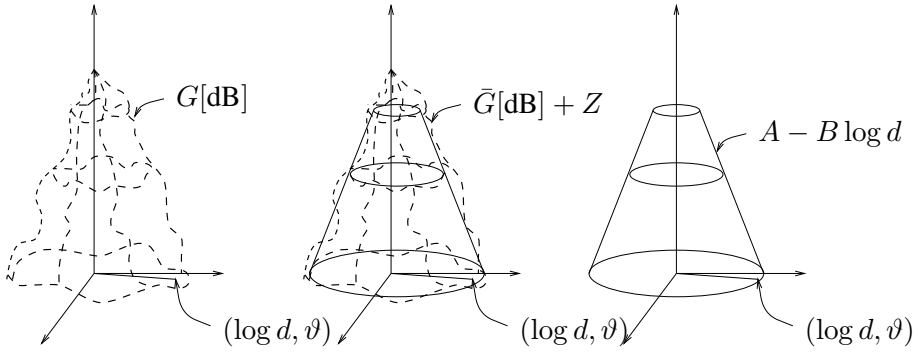

Figure 2.1: The best "cone" fit for $G(d, \vartheta)[\text{dB}]$ and the corresponding error $Z(d, \vartheta)$

2.3 SHADOW FADING

In the previous section, we modeled the mean value of the link gain (in dB) using a few parameters (just A and B in the simplest case). While the mean link gain is modeled as being independent of ϑ, the error term $Z(d, \vartheta)$ in (2.2) is clearly a function of both d and ϑ. We now address the modeling of $Z(d, \vartheta)$. In general, it would be impossible to find a simple parametric deterministic model for the measured values of $Z(d, \vartheta)$. Of course we could always simply interpolate between all the available sample values of $Z(d, \vartheta)$, but such a model will be just as cumbersome as that obtained by interpolating between values of $G(d, \vartheta)$. We hence resort to describing $Z(d, \vartheta)$ using a stochastic model. The error term $Z(d, \vartheta)$, when modelled as stochastic, is called *shadow fading*. Note that since $Z(d, \vartheta)$ is a (random) function in two dimensions, it is a random field. (See Chapter 8 of [WH85] for an introduction to random fields. Also see Appendix C.) We begin our modeling exercise by studying the first order statistics of $Z(d, \vartheta)$.

2.3.1 FIRST ORDER STATISTICS OF SHADOW FADING

Since $Z(d, \vartheta)$ is the residual error obtained from the best curve fit $\bar{G}(d)[\text{dB}]$ to $G(d, \vartheta)[\text{dB}]$, it is reasonable to assume that the average value of $Z(d, \vartheta)$ is zero. Also, assuming that the nature of the environment is roughly isotropic within the coverage of the basestation, the variance of $Z(d, \vartheta)$ may be modeled as being independent of location (d, ϑ). Finally, Central Limit Theorem arguments suggest a Gaussian model for the statistics. Thus, we model $Z(d, \vartheta)$ by a $\mathcal{N}(0, \sigma_Z^2)$ random variable, with the same value of σ_Z^2 for every point in a given region of the cell. This model for $Z(d, \vartheta)$ automatically implies a corresponding model for the multiplicative fading term in (2.1). Since $Z = 10 \log S$, i.e. $S = 10^{Z/10}$, it is easy to show that the pdf of S is given by

$$p_S(s) = \frac{10}{s \ln(10)} \frac{1}{\sigma_Z \sqrt{2\pi}} \exp\left(-\frac{(10 \log s)^2}{2\sigma_Z^2} \right) u(s) \tag{2.4}$$

where $u(\cdot)$ is the unit step function. The distribution of S is called *lognormal* since the logarithm of S is normal (Gaussian), and hence shadow fading is also referred to as lognormal fading.

With the Gaussian model for $Z(d, \vartheta)$, $G(d, \vartheta)[\text{dB}]$ is Gaussian with both mean and median equal to $\bar{G}(d)[\text{dB}]$, and variance σ_Z^2. Hence $G(d, \vartheta)$ is also lognormal. Note that

$$\begin{aligned} \mathsf{E}[G] &= \mathsf{E}\left[10^{\frac{\bar{G}[\text{dB}]+Z}{10}} \right] \\ &< 10^{\frac{\bar{G}[\text{dB}]}{10}} = \bar{G} \end{aligned} \tag{2.5}$$

where the inequality is due to Jensen's inequality [WH85]. Thus the mean of G does not equal $\bar{G}$. However, if we consider the median of G, denoted by μ_G, we see that μ_G is the solution to the equation

$$\begin{aligned} & \mathsf{P}\{G \geq \mu_G\} = \frac{1}{2} \\ \Longrightarrow\ & \mathsf{P}\{10 \log G \geq 10 \log \mu_G\} = \frac{1}{2} \\ \Longrightarrow\ & \mathsf{P}\{G[\text{dB}] \geq \mu_G[\text{dB}]\} = \frac{1}{2} \end{aligned} \tag{2.6}$$

which implies that $\mu_G[\text{dB}] = \bar{G}[\text{dB}]$, since $G[\text{dB}]$ has median $\bar{G}[\text{dB}]$. We summarize this in the following result.

Result 2.1. *The median of G equals $\bar{G}$.*

This is why $\bar{G}(d)$ is sometimes referred to as the *median* link gain.

Thus far we have described only the first order statistics of Z, i.e., the marginal distribution of the shadow fading at a single point (d, ϑ). To completely characterize a random field, it is necessary to specify the joint distribution of any set of sample values of the field. Under a Gaussian field model, all that needs to be specified is the correlation between any given *pair* of sample values of the field.

2.3.2 CORRELATION MODEL FOR SHADOW FADING

To model the field correlation, it is more convenient to use an (x, y) coordinate system, with $x = d\cos\vartheta$ and $y = d\sin\vartheta$. With a slight abuse of notation, we denote the resulting field by $Z(x, y)$. A general model for the field correlation would assume an arbitrary correlation between samples of the field, but such a model would be too cumbersome to be useful. If the scatterers in the cell (or geographical region of interest) are roughly of the same shape and size, it may be reasonable to assume that the correlation between a pair of sample values of the field depends only on the distance between the points and not on their absolute locations.

This leads to the *homogeneous, isotropic*, random field model described in Appendix C. Since $Z(x, y)$ is modelled as Gaussian as well, it is completely characterized by its mean (0 in our model) and correlation function, $R_Z(\Delta)$, which is defined as

$$R_Z(\Delta) = \mathsf{E}[Z(x_1, y_1)\, Z(x_2, y_2)]\,, \quad \text{where } \Delta = \sqrt{(x_2 - x_1)^2 + (y_2 - y_1)^2}. \tag{2.7}$$

What is good model for the correlation function $R_Z(\delta)$? The simplest possible model for the correlation is a "white" model with $R_Z(\delta) = \sigma_Z^2\delta(\Delta)$. However, the white model is clearly unrealistic for shadow fading, since presumably the link gains at points that are close together will be correlated. This leads us to the following first-order correlation model.

Exponential Model for $R_Z(\delta)$

Based on measurements taken in various cities, Gudmundson [Gud91] suggested the following simple exponential correlation model:

$$R_Z(\Delta) = \sigma_Z^2 \exp\left(-\frac{|\Delta|}{D_c}\right), \tag{2.8}$$

where D_c is defined to be the *correlation distance* of the fading process. The value of D_c can be estimated from field trials or detailed simulations. Note that there is no physical justification for this exponential correlation model – it is simply a convenient one parameter function that appears to capture the correlation behaviour observed in field trials. Clearly, a more accurate fit may be obtained by using higher order models with more parameters.

2.3.3 SHADOW FADING IN TIME FOR MOBILE TERMINAL

Consider the situation where one of the terminals is mobile and other is fixed (base) at the origin, with $(x(t), y(t))$ representing the location of the mobile at time t. The power gain of the link sees variations as

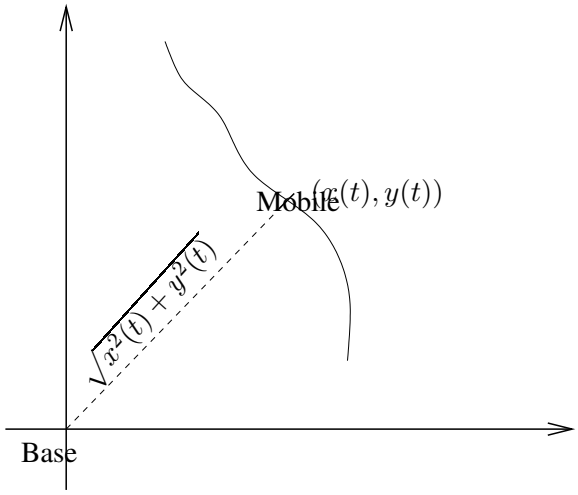

Figure 2.2: Trajectory of mobile terminal.

function of t that are given by

$$G'(t) = \bar{G}\left(\sqrt{x^2(t)+y^2(t)}\right) + Z'(t), \tag{2.9}$$

where $Z'(t) = Z(x(t), y(t))$ is the shadow fading *process* (not field!) seen by the user. Note that

$$\mathsf{E}[Z'(t)Z'(t+\tau)] = R_Z\left(\sqrt{(x(t+\tau)-x(t))^2 + (y(t+\tau)-y(t))^2}\right), \tag{2.10}$$

which means that $Z'(t)$ is, in general, a nonstationary process, even if the field is homogeneous and isotropic.

If the terminal is moving on a straight line with constant velocity v, $Z'(t)$ a stationary process with autocorrelation function

$$\begin{aligned} R_{Z'}(\tau) &= R_Z(v\tau) \\ &= \sigma_Z^2 \exp\left(-\frac{v|\tau|}{D_c}\right) \text{ (for exponential model).} \end{aligned} \tag{2.11}$$

Discrete time (distance) model

Suppose the process $Z'(t)$ is sampled in time such that the k-th sample location is (x_k, y_k). Then the link gain at the k-th sample is given by

$$G_k = \bar{G}\left(\sqrt{x_k^2 + y_k^2}\right) + Z_k, \tag{2.12}$$

where $\{Z_k\}$ is a discrete-time Gaussian process with zero mean, variance σ_Z^2, and autocorrelation function

$$\begin{aligned} R_Z[k, k+m] &= \mathsf{E}[Z_k Z_{k+m}] \\ &= R_Z\left(\sqrt{(x_{k+m}-x_k)^2 + (y_{k+m}-y_k)^2}\right). \end{aligned} \tag{2.13}$$

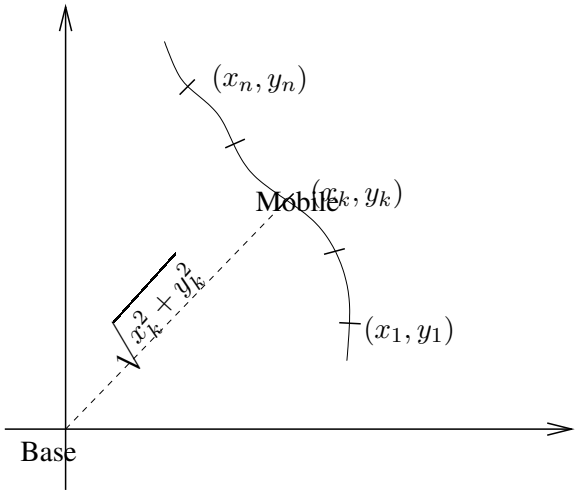

Figure 2.3: Discrete time shadow fading process

If the samples are equally-spaced with distance d_s on a straight line trajectory, then $\{Z_k\}$ is stationary with autocorrelation function

$$\begin{aligned} R_Z[m] &= R_Z(md_s) \\ &= \sigma_Z^2 \exp\left(-\frac{|m|d_s}{D_c}\right) = \sigma_Z^2 a^{|m|} \text{ (for exponential model).} \end{aligned} \tag{2.14}$$

where $a = \exp(-d_s/D_c)$ is the *correlation coefficient* of the process $\{Z_k\}$.

Based on the models we have developed for the large scale variations, we can see that we need a minimum of four parameters (A, B, σ_Z and D_c) to characterize these variations statistically in a region of interest. A piece-wise linear fit for $\bar{G}(d)$ we would require more than one pair (A_i, B_i), and a more accurate correlation model may involve more than just the one parameter D_c.

2.4 SIMULATING LARGE SCALE VARIATIONS

An immediate application of the models we have developed thus far is in the simulation of the large scale variations in a typical cellular environment. To simulate a typical profile for $G(d, \phi)$ over the coverage of a cell, we need to generate the mean $\bar{G}(d)$ and a realization of the random field $Z(d, \phi)$. Generating $\bar{G}(d)$ is easy, especially for a piece-wise linear model in dB. However, generating a set of samples of the shadow fading field $Z(d, \phi)$ is more involved.

2.4.1 SIMULATING THE SHADOW FADING RANDOM FIELD

Consider simulating samples of$Z(d, \phi)$ (or $Z(x, y)$) over some region of interest. Suppose the sample points are $\{(x_i, y_i), i = 1, 2, \ldots, n\}$, and the corresponding field values are:

$$Z_i \stackrel{\Delta}{=} Z(x_i, y_i) \ , \ i = 1, 2, \ldots, n \ . \tag{2.15}$$

Define the vector $\boldsymbol{Z} = [Z_1\ Z_2\ \cdots Z_n]^\top$. Assuming that the field is homogeneous and isotropic with autocorrelation function $R_Z(\delta)$, the covariance matrix $\boldsymbol{\Sigma}$ of $\boldsymbol{Z}$ has components that are given by:

$$\boldsymbol{\Sigma}_{ij} = \mathsf{E}[Z_i Z_j] = R_Z\left(\sqrt{(x_i - x_j)^2 + (y_i - y_j)^2}\right) . \tag{2.16}$$

The random field values can then be jointly generated from a vector $\boldsymbol{W}$ of i.i.d. $\mathcal{N}(0,1)$ random variables as:

$$\boldsymbol{Z} = \boldsymbol{C}\boldsymbol{W}, \tag{2.17}$$

where $\boldsymbol{C}$ is such that $\boldsymbol{C}\boldsymbol{C}^\top = \boldsymbol{\Sigma}$. One way to obtain $\boldsymbol{C}$ is through an LU decomposition [HJ85] of $\boldsymbol{\Sigma}$.

2.4.2 SIMULATING THE SHADOW FADING PROCESS

In the special case, where we are interested in simulating the discrete-time shadow fading process when the is mobile moving through the cell with a constant velocity, the problem is considerably easier. To simulate the discrete time process $\{Z_k\}$ for a stationary model with autocorrelation function $R_Z[m]$, we simply filter a sequence $\{W_k\}$ of i.i.d. $\mathcal{N}(0,1)$ random variables (white Gaussian noise) through a LTI system. The filter transfer function $H(z)$ must satisfy

$$H(z)H(z^{-1}) = S_Z(z)\,, \tag{2.18}$$

where $S_Z(z)$ is the Z-transform of $R_Z[m]$. Such a filter can be found by *spectral factorization* [WH85].

For the exponential autocorrelation function $R_Z[m] = \sigma_Z^2 a^{|m|}$,

$$S_Z(z) = \frac{\sigma_Z^2(1-a^2)}{(1-az^{-1})(1-az)}\,, \tag{2.19}$$

which implies that

$$H(z) = \frac{\sigma_Z\sqrt{1-a^2}}{1-az^{-1}}\,. \tag{2.20}$$

Thus $\{Z_k\}$ can be calculated using the recursive equations:

$$\begin{aligned} Z_0 &= \sigma_Z W_0 \\ Z_{k+1} &= aZ_k + \sigma_Z\sqrt{1-a^2}W_{k+1},\ \ k = 0,1,\ldots \end{aligned} \tag{2.21}$$

In this case, the sequence $\{Z_k\}$ is also referred to as a first-order autoregressive (AR-1) discrete-time stochastic process [WH85].

2.5 APPLICATIONS OF LARGE SCALE FLUCTUATION MODELS

The first two applications discussed below use only the first-order statistics of shadow fading, whereas the last one uses correlation information as well.

2.5.1 CELLULAR AREA RELIABILITY

Consider the design of a cellular basestation network. If the transmit power is P_t [dBm], then the received power at (d, ϑ) is given by

$$\begin{aligned} P_r(d,\vartheta)\,[\text{dBm}] &= P_t\,[\text{dBm}] + G(d,\vartheta)\,[\text{dB}] \\ &= P_t\,[\text{dBm}] + A - B\log d + Z(d,\vartheta) \\ &= A_t - B\log d + Z(d,\vartheta)\ . \end{aligned} \tag{2.22}$$

where $A_t = P_t\,[\text{dBm}] + A$.

The cells are to be designed in such a way that received signal strength is at a reliable level over the coverage of the cell. The probability of outage at a point (d, ϑ) is defined to be the probability that $P_r(d, \vartheta)$ [dBm] falls below a threshold P_{th} [dBm] required for reliable performance, i.e.,

$$\mathsf{P}_{\text{out}}(d,\vartheta) = \mathsf{P}\left\{A_t - B\log d + Z(d,\vartheta) < P_{\text{th}}\,[\text{dBm}]\right\}\ . \tag{2.23}$$

Since Z is Gaussian with mean zero and variance σ_Z, we have

$$\mathsf{P}_{\text{out}}(d,\vartheta) = 1 - Q\left(P_{\text{th}}\,[\text{dBm}] - A_t + B\log d\right)\ , \tag{2.24}$$

where $Q(\cdot)$ is the tail of unit Gaussian distribution, i.e.,

$$Q(x) = \frac{1}{\sqrt{2\pi}}\int_x^\infty e^{-\frac{x^2}{2}}\,dx\ . \tag{2.25}$$

The *area reliability* of the cell [Rap96] is defined by

$$\begin{aligned} F_{\text{area}} &= 1 - \text{average outage probability over the cell} \\ &= 1 - \frac{1}{\pi R^2}\int_0^R\int_{-\pi}^{\pi}\mathsf{P}_{\text{out}}(\rho,\vartheta)\rho\,d\rho\,d\vartheta\ . \end{aligned} \tag{2.26}$$

where R is the cell radius.

From (2.24) and (2.26), it follows that

$$F_{\text{area}} = \frac{2}{R^2}\int_0^R Q(a + b\ln\rho)\rho\,d\rho, \tag{2.27}$$

where a and b are given by

$$a = \frac{P_{\text{th}}\,[\text{dBm}] - A_t}{\sigma_Z}, \quad b = \frac{B}{\sigma_Z\ln(10)}\ . \tag{2.28}$$

It is a straightforward exercise in integration by parts to show that

$$F_{\text{area}} = Q(a + b\ln R) + \frac{\exp\left(\frac{2}{b^2} - \frac{2a}{b}\right)}{R^2}\left[1 - Q\left(a + b\ln R - \frac{2}{b}\right)\right]\ . \tag{2.29}$$

A related quantity of interest in characterizing the reliability in a cell is the *edge reliability*, F_{edge}, which is defined by

$$F_{\text{edge}} = 1 - \mathsf{P}_{\text{out}}(R) = Q(a + b\ln R)\ . \tag{2.30}$$

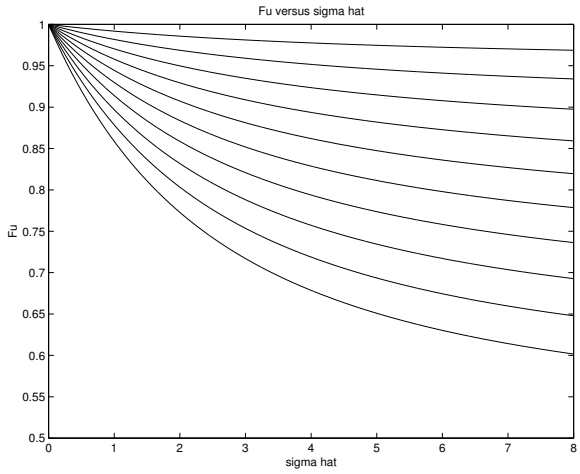

Figure 2.4: Area reliability as a function of edge reliability and normalized shadow fading standard deviation.

It easy to show that F_{edge} and F_{area} are related in the following manner:

$$F_{\text{area}} = F_{\text{edge}} + e^{\frac{2}{b^2}} e^{-\frac{2}{b}Q^{-1}(F_{\text{edge}})} \left(1 - Q\left(Q^{-1}(F_{\text{edge}}) - \frac{2}{b}\right)\right) \tag{2.31}$$

For fixed F_{edge}, F_{area} is independent of a and R, and is a function of b only. This means that once we fix the edge reliability to a desired value, then the area reliability is only a function of the pathloss exponent $B/10$ and the shadow fading standard deviation σ_Z. If we define the normalized standard deviation by

$$\hat{\sigma}_Z = \frac{10\sigma_Z}{B} \tag{2.32}$$

then F_{area} can be expressed in terms of F_{edge} and $\hat{\sigma}_Z$ using (2.31). This relationship is captured in Figure 2.4.

2.5.2 SIR IN CHANNELIZED SYSTEMS WITH SHADOW FADING

In channelized (F/TDMA) cellular communication systems, the signal-to-interference ratio (SIR) seen by a user in the cell of interest is given by

$$\Gamma = \frac{P_{r,0}}{\sum_{i=1}^{N_I} P_{r,i}} , \tag{2.33}$$

where $P_{r,0}$ is the power received from the transmitter of interest, $P_{r,i}$ is the power received from the i-th co-channel interferer, and N_I is the number of co-channel interferers.

If we consider the downlink (basestation to mobile), then with the received power at location (d, ϑ) relative to the basestation modeled as in (2.22), it is easy to see that

$$P_r(d, \vartheta) = K d^{-n} S(d, \vartheta) , \tag{2.34}$$

where $K = 10^{A_t/10}$ and $n = B/10$.

Assuming that median gain parameters (A and B) and the transmit powers (P_t) are the same for basestations, K and n are equal for all basestations. If we compute the SIR of(2.33) after averaging out the small scale variations from the received powers, then

$$\Gamma \;=\; \frac{S_0 D_0^{-n}}{\sum_{i=1}^{N_I} S_i D_i^{-n}} \;=\; \frac{S_0}{\sum_{i=1}^{N_I} S_i \left(\frac{D_i}{D_0}\right)^{-n}}, \tag{2.35}$$

where S_0 is the (lognormal) shadow fading seen on the link from the intended basestation, and S_i is the fading seen from the i-th cochanell interferer. Also, D_0 is the distance to the intended basestation, and D_i is the distance to the i-th co-channel interferer.

If we model $S_0, S_1, S_2, \ldots, S_{N_I}$ as independent random variables, then the sum in the denominator of (2.35) can be approximated reasonably well by a lognormal[1]. This leads to a lognormal model for Γ (since the ratio of lognormals is lognormal) whose statistics can be determined explicitely. To do this we use the following result that is easily established from first principles.

Result 2.2. *Suppose X is a lognormal random variable with mean m_X and second moment δ_X, and suppose $Y = 10\log X$ has mean m_Y and variance σ_Y^2. (Note that Y is Gaussian.)*

$$\begin{aligned} m_X &= \exp\left(\frac{(\beta\sigma_Y)^2}{2}\right)\exp(\beta m_Y), \\ \delta_X &= \exp\left(2(\beta\sigma_Y)^2\right)\exp(2\beta m_Y), \\ m_Y &= 20\log m_X - 5\log\delta_X, \\ \sigma_Y^2 &= \frac{1}{\beta}(10\log\delta_X - 20\log m_X), \end{aligned} \tag{2.36}$$

where $\beta = \ln(10)/10$.

Example: SIR for single tier crude approximation.

Consider the first tier of six cochannel interfering cells surrounding the cell of interest in a hexagonal cellular grid. If only these interferers are included in the SIR calculation, then the worst-case SIR can be approximated as [Rap96]:

$$\Gamma_{\text{worst-case}} \approx \frac{S_0 R^{-n}}{\sum_{i=1}^{6} S_i D_i^{-n}} \approx \left(\frac{D}{R}\right)^n \frac{S_0}{\sum_{i=1}^{6} S_i} \tag{2.37}$$

where D is the distance between cochannel cells, and R is the cell radius.

Let $S_T = \sum_{i=1}^{6} S_i$. For the lognormal approximation we need to compute m_{S_T} and δ_{S_T}, which are given by:

$$\begin{aligned} m_{S_T} &= \sum_{i=1}^{6} m_{S_i}\ , \\ \delta_{S_T} &= m_{S_T}^2 + \sum_{i=1}^{6}\left[\delta_{S_i} - m_{S_i}^2\right]\ . \end{aligned} \tag{2.38}$$

[1] More accurate approximations can be derived (see Section 3.1 of Stuber [Stu96]).

Now suppose the $\{S_i\}$ are identically distributed, with $Z_i = 10 \log S_i \sim \mathcal{N}(0, \sigma^2)$. Then it is easy to show from (2.36) that

$$\begin{aligned} m_{S_T} &= 6 \exp\left(\frac{\beta^2 \sigma^2}{2}\right) , \\ \delta_{S_T} &= 6 \left[\exp\left(2\beta^2\sigma^2\right) + 5\exp(\beta^2\sigma^2)\right] \end{aligned} \tag{2.39}$$

and that $Z_T = 10 \log S_T$ is Gaussian with

$$\begin{aligned} m_{Z_T} &= 20 \log m_{S_T} - 5 \log \delta_{S_T}, \\ \sigma^2_{Z_T} &= \frac{1}{\beta}(10 \log \delta_{S_T} - 20 \log m_{S_T}) . \end{aligned} \tag{2.40}$$

Note that $m_{Z_T} \neq 0$. Now let $\tilde{\Gamma}$ be the SIR in dB. Then from (2.37), we get

$$\tilde{\Gamma} = 10n \log\left(\frac{D}{R}\right) + Z_0 - Z_T \tag{2.41}$$

This means that $\tilde{\Gamma}$ is Gaussian with

$$\begin{aligned} m_{\tilde{\Gamma}} &= 10n \log\left(\frac{D}{R}\right) - m_{Z_T} , \\ \sigma^2_{\tilde{\Gamma}} &= \sigma^2 + \sigma^2_{Z_T} . \end{aligned} \tag{2.42}$$

We can now pose a question such as: what is the probability that the worst-case SIR is less than 18 dB? The answer is easily seen to be $1 - Q((18 - m_\epsilon)/\sigma_\epsilon)$, which can be computed terms of D, R, n and σ^2 using the series of equations derived above.

2.5.3 SIGNAL STRENGTH PREDICTION

For radio resource management functions (such as handoff and power control) in cellular systems, it is often of interest to be able to predict the large scale variations of the channel based on previous measurements. These measurements may, for example, be available through monitoring of pilot signals.

Suppose k sample values of the signal strength at locations $(d_1, \vartheta_1), \ldots, (d_k, \vartheta_k)$ are known, and using these values we wish to predict the signal strength at location $(d_{k+1}, \vartheta_{k+1})$. Now, the received power for sample i, $1 \leq i \leq k$ is given by

$$P_{r,i} = A_t - B \log d_i + Z_i. \tag{2.43}$$

If we assume that A_t, B and the d_i's are known, the problem of predicting $P_{r,k+1}$ based on $P_{r,1}, \ldots, P_{r,k}$ is equivalent to that of predicting Z_{k+1} based on $Z_1, \ldots, Z_k$.

The prediction problem can be posed in a minumum mean squared-error (MMSE) framework. Under the Gaussian model for the Z_i's, the MMSE predictor for Z_{k+1} is linear and is given by

$$\hat{Z}^{\text{MMSE}}_{k+1} = \sum_{i=1}^{k} a_i Z_i, \tag{2.44}$$

where the a_i's are solutions to the Yule-Walker equations [WH85]:

$$\begin{bmatrix} R_{1,1} & R_{1,2} & \dots & R_{1,k} \\ R_{2,1} & R_{2,2} & \dots & R_{2,k} \\ \vdots & \vdots & \vdots & \vdots \\ R_{k,1} & R_{k,2} & \dots & R_{k,k} \end{bmatrix} \begin{bmatrix} a_1 \\ a_2 \\ \vdots \\ a_k \end{bmatrix} = \begin{bmatrix} R_{1,k+1} \\ R_{2,k+1} \\ \vdots \\ R_{k,k+1} \end{bmatrix} \tag{2.45}$$

with $R_{i,j} = \mathsf{E}[Z_i Z_j]$, which can be computed based on knowledge of the field autocorrelation function $R_Z(\Delta)$.

The MMSE solution takes on a much simpler form in the special case where the samples $\{Z_k\}$ form an AR-1 process (see Section 2.4.2). In this case it easy to see that

$$\hat{Z}_{k+1}^{\text{MMSE}} = \mathsf{E}[Z_{k+1} \mid Z_k, \dots, Z_1] = aZ_k \tag{2.46}$$

and also that

$$\hat{P}_{r,k+1}^{\text{MMSE}} = aP_{r,k} + (1-a)A_t - B\log\left(\frac{d_{k+1}}{d_k^a}\right) . \tag{2.47}$$

2.6 CONCLUDING REMARKS

In this chapter we developed a model for the variations in the power gain in a terrestrial cellular system as a function of the location of the receiver relative to the transmitter. We saw that is was possible to characterize the variations stochastically using a few parameters. We note that in addition to variations in power gain, there may be other large-scale variations in the channel introduced by mobility. In Chapter 3, we will see that the small scale variations in the channel are a function of the Rice factor, which is strength of the line-of-sight path relative to the diffuse reflected paths connecting the Tx and Rx antennas. The variations in the Rice factor are sometimes modelled using a lognormal distribution. We will also see in Chapter 3, that the time and frequency selectivity of the channel depend on the delay-Doppler scattering function of the channel, which is a description of the distribution of received power as a function of delay and Doppler frequency. The delay-Doppler scattering function depends of the location of the mobile and the varies over the large scale. The same is true of the spatial scattering function that is studied in Chapters 5. Modeling variations in the scattering functions is a difficult and open problem that deserves further attention.

Chapter 3

Small scale Variations in Gain

3.1 INTRODUCTION

In Chapter 1 we justified the separation of the variations in the channel into two scales, and in Chapter 2 we studied the large scale variations in the channel. In this chapter, we study the small scale variations, treating the large scale variations as constant (see Fig 3.1). Our analysis here is restricted to the situation where only one antenna is present at the transmitter and receiver. Generalizations are considered in Chapter 5.

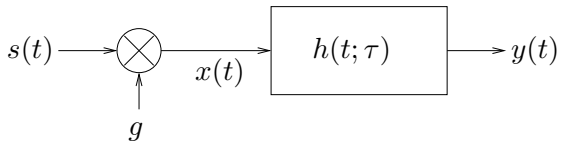

Figure 3.1: Small scale variations in the channel (with large scale variations treated as constant)

Recall from Section 1.3 that the small scale variations in the channel are captured in a linear system with response

$$h_{d,\vartheta}(\tau) = \sum_{n=1}^{N} \beta_n(d,\vartheta)\, e^{j\phi_n(d,\vartheta)}\, \delta(\tau - \tau_n(d,\vartheta)) \tag{3.1}$$

where the gains $\{\beta_n\}$ are normalized so that $\sum_{n=1}^{N} \beta_n^2 = 1$. Small movements of the terminals (around relative location (d,ϑ)), or movements of the scatterers, cause the gains $\{\beta_n\}$, the delays $\{\tau_n\}$ and the phases $\{\phi_n\}$ to vary with time. Thus the channel corresponding to the small scale variations becomes time-varying, with an impulse response that is given by

$$h(t;\tau) = \sum_{n=1}^{N} \beta_n(t)\, e^{j\phi_n(t)}\, \delta(\tau - \tau_n(t)) \tag{3.2}$$

For notational convenience, from here foreword, we will skip the number of paths, N, in the summations.

Treating the large scale variations $g(d, \vartheta)$ as roughly constant (see Figure 3.1), we obtain the input-output relationship:

$$\begin{aligned} y(t) &= \int_0^\infty h(t;\tau)x(t-\tau)d\tau \\ &= g \int_0^\infty h(t;\tau)s(t-\tau)d\tau \ . \end{aligned} \tag{3.3}$$

3.2 DELAY POWER PROFILE AND DELAY SPREAD

As we remarked earlier in Chapter 1, for movements of the order of a few wavelengths, $\{\beta_n(t)\}$ and $\{\tau_n(t)\}$ can be assumed to be roughly constant, and the time variations in $h(t;\tau)$ are mainly due to changes in $\{\phi_n(t)\}$, i.e.,

$$h(t;\tau) \approx \sum_n \beta_n \, e^{j\phi_n(t)} \, \delta(\tau - \tau_n) \tag{3.4}$$

The power gain associated with the n-th path is given by β_n^2. One way to describe the physical scattering environment for the purposes of studying the channel is to plot the power gains in the paths as a function of the delay. Such a plot, which is shown in Figure 3.2, is called the *delay power profile* (or simply *delay profile*) of the channel. Notice that we have associated an impulse or delta function with each path in Figure 3.2. The reason is that the power delay profile can be also interpreted as a power gain density as a function of delay since we have normalized the powers in the paths to add up to unity.

With some possible abuse of notation, we use the index 0 to denote the line of sight (LOS) path, if one exists. The width of the delay profile (delay spread) is of the order of tens of microseconds for outdoor channels, and of the order of hundreds of nanoseconds for indoor channels. Note that the paths typically appear in clusters in the delay profile, with each cluster representing a diffuse reflector.

Definition 3.1. *The quantity $\tau_{ds} = \max \tau_n - \min \tau_n$ is called the delay spread of the scattering environment seen by the terminals.*

Without loss of generality, we may assume that the delay corresponding to the first path arriving at the receiver is 0. The first path would of course be the LOS path if one exists. Then $\min \tau_n = 0$, $\tau_{\text{ds}} = \max \tau_n$, and (3.3) can be rewritten as:

$$\begin{aligned} y(t) &= \int_0^{\tau_{\text{ds}}} h(t;\tau)x(t-\tau)d\tau \\ &= g \int_0^{\tau_{\text{ds}}} h(t;\tau)s(t-\tau)d\tau \end{aligned} \tag{3.5}$$

The delay profile is the key to characterizing the frequency selectivity of the channel as we shall see in Section **??**.

3.3 DOPPLER POWER PROFILE AND DOPPLER SPREAD

As we remarked earlier, the time variations on the small scale are entirely due to variations in the path phases. To understand the nature of these variations, consider the simple scenario where only one of the terminals is

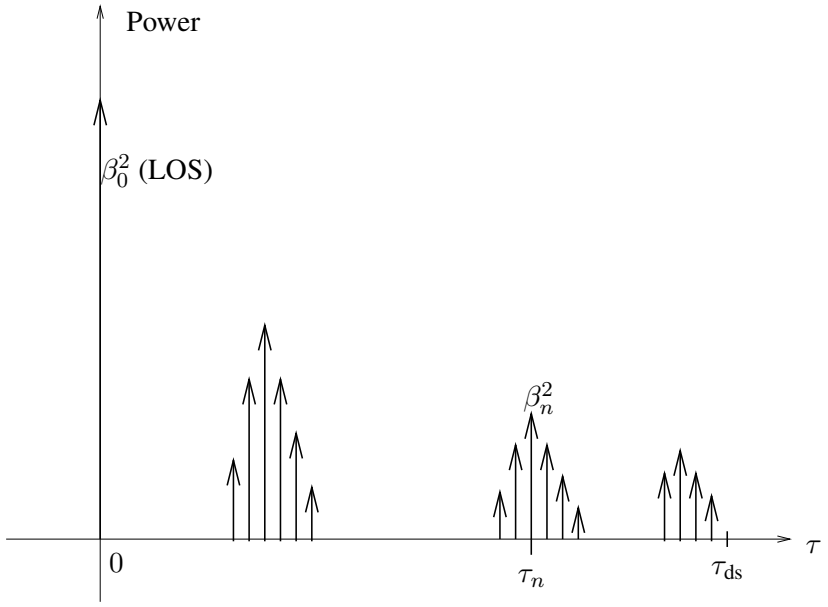

Figure 3.2: Typical delay power profile of channel with LOS path having delay 0.

mobile and the scatterers are fixed. Suppose the mobile is traveling with velocity v and suppose that the n-th path has an angle of arrival $\theta_n(t)$ with respect to the velocity vector as shown in Figure 3.3. The angle of arrival $\theta_n(t)$ plays a key role in the phase variations. Note that we may assume that θ_n is roughly constant over the small scale. Then for small Δ_t,

$$\phi_n(t+\Delta_t) - \phi_n(t) \approx \frac{2\pi f_c v \Delta_t \cos\theta_n}{c} = \frac{2\pi v}{\lambda_c}\ \Delta_t\ \cos\theta_n\ , \tag{3.6}$$

where λ_c is the carrier wavelength and c is the velocity of light. The frequency shift in the n-th path introduced by the movement of the mobile is hence given by

$$\nu_n = \lim_{\Delta_t \to 0} \frac{\phi_n(t+\Delta_t) - \phi_n(t)}{2\pi\Delta_t} = \frac{v}{\lambda_c}\cos\theta_n \tag{3.7}$$

This frequency shift is familiar *Doppler shift* that is commonly observed in the context of sound waves travelling from moving sources.

More generally, both terminals and the scatterers may be mobile. In this case, the phase shift introduced in the n-path will be due all the mobile units (terminals and scatterers) contributing to the path. Over the small scale it is reasonable to assume that all mobile units are travelling at constant velocities. Hence the phase difference term shown in (3.6) gets modified as:

$$\phi_n(t+\Delta_t) - \phi_n(t) \approx \sum_{i=1}^{M}\ \frac{2\pi v_i}{\lambda_c}\ \Delta_t\ \cos\theta_{n,i}\ , \tag{3.8}$$

where M is the number of mobile units, v_i is the velocity of the i-th mobile unit relative to the previous unit in the path and $\theta_{n,i}$ is the angle of arrival at the i-th unit. The corresponding frequency shift is given by:

$$\nu_n = \sum_{i=1}^{M}\ \frac{v_i}{\lambda_c}\ \cos\theta_{n,i}\ . \tag{3.9}$$

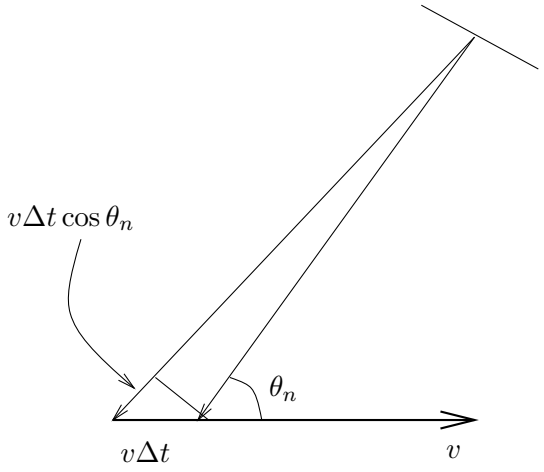

Figure 3.3: Doppler Shift.

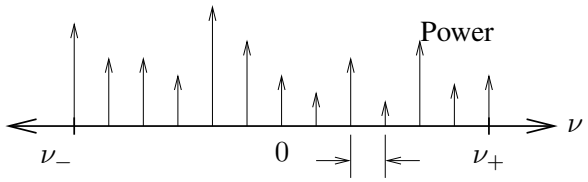

Figure 3.4: Doppler power profile.

Note that if the maximum possible velocity for the mobile units is $v_{\max}$, then the Doppler shift for any path is upper bounded by $\nu_{\max} = 2v_{\max}/\lambda_c$.

Just as we plotted the power in the paths as a function of their delay, we may also plot the power in the paths as a function of the Doppler shift associated with them. An example *Doppler power profile* (or simply *Doppler profile*) of the channel is shown in Figure 3.4. Again, we associate an impulse with each path in the Doppler profile, with the understanding that the profile can also be interpreted as a power gain density as a function of Doppler shift. We will revisit this interpretation in Section 3.4.1.

We denote the minimum and maximum Doppler frequency (for a given location of the terminals) by ν_- and ν_+, respectively, with

$$\nu_- = -\min_n \nu_n \,, \quad \nu_+ = \max_n \nu_n \,. \tag{3.10}$$

We then have the following definition of Doppler spread that is analogous to the delay spread of Definition 3.1.

Definition 3.2. *The quantity $\nu_{ds} = \nu_+ - \nu_-$ is called the Doppler spread of the scattering environment seen by the terminals.*

Unlike in the case of the delay profile, we do not change the axes in the Doppler profile to obtain a profile that spans the range of Doppler frequencies $[0, \nu_{\text{ds}}]$. This is because the actual value of the Doppler shift is important in the determining how the carrier frequency is affected by the phase variations introduced by channel.

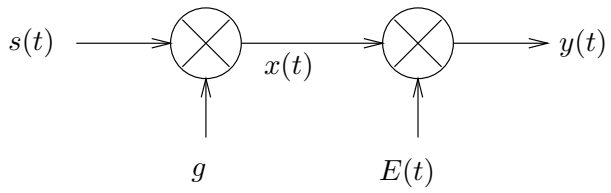

Figure 3.5: Channel Model for Flat Fading

The Doppler power profile will play a key role in characterizing the time selectivity of the channel as we shall see in following section.

3.4 PURELY TIME-SELECTIVE (FREQUENCY-FLAT) FADING

If the bandwidth of transmitted signal $s(t)$ is much smaller than $1/\tau_{\text{ds}}$, then $s(t)$, and hence the input $x(t)$, does not change much over time intervals of the order of τ_{ds}. Thus (3.5) can be approximated as

$$y(t) \approx x(t) \int_0^{\tau_{\text{ds}}} h(t;\tau) d\tau = x(t) \sum_n \beta_n e^{j\phi_n(t)} \, . \tag{3.11}$$

This implies that the multipath channel simply scales the transmitted signal without introducing significant frequency distortion. The variations with time of this scale factor are referred to as frequency nonselective, or *flat*, fading.

Note that the distortions introduced by the channel depend on the relationship between the delay spread of the channel and the bandwidth of the signal. The same channel may be frequency selective or flat, depending on the bandwidth of the input signal. With a delay spread of 10 μs corresponding to a typical outdoor urban environment, an analog AMPS signal (30 kHz) undergoes flat fading, whereas an IS-95 CDMA signal (1.25 MHz) undergoes frequency selective fading.

For flat fading, the channel of Figure 3.1 simplifies to that shown in Figure 3.5, i.e.,

$$y(t) = E(t) \; x(t) \, , \tag{3.12}$$

where

$$E(t) = \int_0^{\tau_{\text{ds}}} h(t;\tau) d\tau = \sum_n \beta_n \, e^{j\phi_n(t)} \, . \tag{3.13}$$

3.4.1 STATISTICAL CHARACTERIZATION OF FLAT FADING

To model $E(t)$ statistically, we first fit a stochastic model to the phases $\{\phi_n(t)\}$. Based on the Doppler model for the phase drift given in (3.8), we may approximate the evolution of the phase process as

$$\phi_n(t) \approx \varphi_n + 2\pi\nu_n t \tag{3.14}$$

where φ_n is an initial phase.

We may combine the initial phase with the path gain to define the *complex path gain*

$$\alpha_n = \beta_n \, e^{j\varphi_n} \, . \tag{3.15}$$

Furthermore, we define the complex path process $e_n(t)$ as

$$e_n(t) = \alpha_n \, e^{j2\pi\nu_n t} \tag{3.16}$$

so that

$$E(t) = \sum_n e_n(t) \, . \tag{3.17}$$

The randomness in $E(t)$ is captured in the initial phases $\{\varphi_n\}$, which we model using the following reasonable assumption.

Assumption 3.1. *For each n, the initial phase φ_n is a random variable that is uniformly distributed on $[-\pi, \pi]$.*

This assumption immediately gives us the result that the path process $e_n(t)$ is a zero mean process. Furthermore, using (3.17), we obtain the following important result.

Result 3.1. *$E(t)$ is a zero-mean process.*

The uniform phase assumption actually yields an even more powerful result about the process $E(t)$. In particular, the pseudocovariance function of $e_n(t)$ can be computed as follows.

$$\begin{aligned} \tilde{C}_{e_n}(t+\xi, t) &= \mathsf{E}[e_n(t) e_n(t+\xi)] \\ &\approx \beta_n^2 \mathsf{E}[e^{j(2\varphi_n + 2\pi\nu_n(2t+\xi))}] = 0 \end{aligned} \tag{3.18}$$

where the approximation follows from (3.14). This implies that $e_n(t)$ is (approximately) a proper complex random process (see Definition B.2 in Appendix B). Furthermore, using the result that linear combinations of proper complex processes remain proper (see Result B.5 Appendix B), we obtain:

Result 3.2. *The process $E(t)$ is (approximately) a proper complex random process.*

It is worth pointing out that standard analyses of the fading processes (see, e.g., [Jak74, Pro95, Stu96]) do not fully exploit the properness of the process $E(t)$. The statistical properties of the fading process are instead established by considering the inphase and quadrature components separately. By establishing that $E(t)$ is proper at the start, we will see that the subsequent analysis is much simplified and cleaner.

Thus far we have established that $E(t)$ is a zero mean proper complex process. In order to characterize the autocorrelation function of $E(t)$, we need to know how the phases $\{\varphi_n\}$ are jointly distributed. This leads us to the most important assumption of this book.

Assumption 3.2. *The initial phases $\{\varphi_n\}$ of the different paths are independent random variables.*

This assumption together with Assumption 3.1 implies the following results:

$$\mathsf{E}[e^{j\varphi_n} \, e^{-j\varphi_{n'}}] = \delta[n - n'], \quad \text{and } \mathsf{E}[e^{j\varphi_n} \, e^{j\varphi_{n'}}] = 0 \tag{3.19}$$

where $\delta[\cdot]$ is the discrete Dirac function.

We can now compute the autocorrelation function of the proper complex process $E(t)$ as follows:

$$\begin{aligned} R_E(t+\xi,t) &= \mathsf{E}\left[E(t+\xi)E^{\star}(t)\right] \\ &= \mathsf{E}\left[\sum_n \beta_n\, e^{j\varphi_n+2\pi\nu_n(t+\xi)} \sum_{n'} \beta_{n'}\, e^{-j\varphi_{n'}-2\pi\nu_{n'}t}\right] \\ &= \sum_n \beta_n^2\, \mathsf{E}\left[\, e^{j2\pi\nu_n\xi}\right] \quad \text{(by (3.19))} \\ &= \sum_n \beta_n^2\, e^{j2\pi\nu_n\xi} \stackrel{\Delta}{=} R_E(\xi) \end{aligned} \tag{3.20}$$

This of course implies that $E(t)$ is wide sense stationary.

Result 3.3. *The process $E(t)$ may be modelled as a zero-mean, wide sense stationary, proper complex process over short time horizons corresponding to movements of the order of a few wavelengths in distance, with autocorrelation function*

$$R_E(\xi) = \sum_n \beta_n^2\, e^{j2\pi\nu_n\xi} \tag{3.21}$$

In-Phase and Quadrature Processes

From (3.13) it is clear that the in-phase and quadrature processes $E_I(t)$ and $E_Q(t)$ are given by

$$E_I(t) = \sum_n \beta_n \cos\phi_n(t), \;\; \text{and } E_Q(t) = \sum_n \beta_n \sin\phi_n(t)\,. \tag{3.22}$$

It is possible to compute the auto- and cross-correlation functions of $E_I(t)$ and $E_Q(t)$ from scratch using (3.22) as is done, for example, in [Pro95, Stu96]. However, if we exploit the fact that $E(t)$ is a proper process, we immediately have (see (B.12)):

$$\begin{aligned} R_{E_I}(\xi) = R_{E_Q}(\xi) &= \frac{1}{2}\,\mathsf{Re}\left\{R_E(\xi)\right\} \\ &= \frac{1}{2}\,\sum_n \beta_n^2 \cos(2\pi\nu_n\xi)\,, \end{aligned} \tag{3.23}$$

and that

$$\begin{aligned} R_{E_QE_I}(\xi) = -R_{E_IE_Q}(\xi) &= \frac{1}{2}\,\mathsf{Im}\left\{R_E(\xi)\right\} \\ &= \frac{1}{2}\,\sum_n \beta_n^2 \sin(2\pi\nu_n\xi)\,. \end{aligned} \tag{3.24}$$

Dopper Power Density and Continuum-of-Paths Model

We mentioned earlier in Section 3.3 that the Doppler profile can also be interpreted as a power (gain) density as a function of Doppler shift, since the power gains $\{\beta_n^2\}$ have been normalized so that $\sum_n \beta_n^2 = 1$. This leads to the following definition.

Definition 3.3. *The Doppler power density $\Psi(\nu)$ is given by*

$$\Psi(\nu) = \sum_n \beta_n^2 \, \delta(\nu - \nu_n) \, . \tag{3.25}$$

Clearly, as is implied from the term density,

$$\int_{-\nu_-}^{\nu_+} \Psi(\nu) \, d\theta = 1 \tag{3.26}$$

We can now express the autocorrelation function of $E(t)$ in terms of $\Psi(\nu)$. From (3.21) it is easy to see that

$$R_E(\xi) = \int_{-\nu_-}^{\nu_+} \Psi(\nu) e^{j2\pi\nu\xi} d\nu \, . \tag{3.27}$$

Furthermore, the auto- and cross-correlation function of the inphase and quadrature components can be written as

$$\begin{aligned} R_{E_I}(\xi) = R_{E_Q}(\xi) &= \frac{1}{2} \int_{-\nu_-}^{\nu_+} \Psi(\nu) \cos(2\pi\nu\xi) d\nu \, , \\ R_{E_Q E_I}(\xi) = -R_{E_I E_Q}(\xi) &= \frac{1}{2} \int_{-\nu_-}^{\nu_+} \Psi(\nu) \sin(2\pi\nu\xi) d\nu \, . \end{aligned} \tag{3.28}$$

We may also approximate the discrete density of (3.25) by a continuous density and think of the paths as forming a *continuum*. The continuous model serves as a good approximation to diffuse scattering that we will study below in Section 3.4.2. Another justification for the model is that any practical method to measure/estimate the Doppler profile of the environment will be limited in resolution due to finite windowing in time, and hence impulses in the Doppler power density will be smoothed out by the measurement process.

It is also clear from (3.27) that $\Psi(\nu)$ is the Fourier transform of the $R_E(\xi)$, i.e., that Ψ is the power spectral density of the fading process $E(t)$:

$$S_E(\nu) = \Psi(\nu) \, . \tag{3.29}$$

This is why the Doppler power density is also called the Doppler power *spectral* density.

To understand how the Doppler power density manifests itself in the fading channel consider the simple case where the passband transmitted signal $\tilde{s}(t)$ is a pure carrier without any modulating message signal, i.e., $\tilde{s}(t) = \cos(2\pi f_c t)$. Then $s(t) = 1$ and $y(t) = gE(t)$ (see Figure 3.5). Now consider the passband process $\tilde{y}(t)$ corresponding to baseband process $y(t)$. Since $y(t)$ is a proper complex process, it follows from (1.6) that

$$R_{\tilde{y}}(\xi) = \text{Re}\left[R_y(\xi) \, e^{j2\pi f_c \xi}\right] = g^2 \text{Re}\left[R_E(\xi) \, e^{j2\pi f_c \xi}\right] \, , \tag{3.30}$$

and hence that

$$\begin{aligned} S_{\tilde{y}}(f) &= \frac{g^2}{2} \left[S_E(f - f_c) + S_E(-f - f_c)\right] \\ &= \frac{g^2}{2} \left[\Psi(f - f_c) + \Psi(-f - f_c)\right] \end{aligned} \tag{3.31}$$

This means that the single tone at the carrier frequency is spread out over the range of frequencies defined by the Doppler power density.

Special Case of Single Mobile Terminal

For a general $\Psi(\nu)$, the integrals in (3.27) and (3.28)) cannot be obtained in closed form. Let us now consider a special scenario where only one of the terminals is mobile with velocity v, and the scatterers are fixed. This is a reasonable model for certain suburban cellular environments. In this case the Doppler shift along each path n is completely determined by the angle θ_n of made by the path at the mobile terminal as shown in Figure 3.3. In particular

$$\nu_n = \nu_{\max} \cos\theta_n \tag{3.32}$$

where $\nu_{\max} = v/\lambda_c$. Furthermore, $\nu_+ = -\nu_- = \nu_{\max}$.

Since the path angles the mobile determine the time variations in the channel, it is of interest to study the distribution of power with the angle. To this end we have the following definition.

Definition 3.4. *The Angular power density $\gamma(\theta)$ is given by*

$$\gamma(\theta) = \sum_n \beta_n^2 \, \delta(\theta - \theta_n) \, . \tag{3.33}$$

The Doppler power density and the angular power density are related via change of variables as:

$$\Psi(\nu) = \begin{cases} \dfrac{\gamma(\cos^{-1}(\nu/\nu_{\max})) + \gamma(-\cos^{-1}(\nu/\nu_{\max}))}{\sqrt{\nu_{\max}^2 - \nu^2}} & \text{for } |\nu| < \nu_{\max} \\ 0 & \text{otherwise} \end{cases} \tag{3.34}$$

Note also that we can rewrite (3.27) in terms of $\gamma(\theta)$ as:

$$R_E(\xi) = \int_{-\nu_{\max}}^{\nu_{\max}} \gamma(\theta) e^{j2\pi\nu_{\max}\xi\cos\theta} d\theta \, . \tag{3.35}$$

We can rewrite (3.28) similarly.

Now, consider the situation where the propagation environment is such that power is distributed roughly uniformly over angles at the mobile terminal. We may approximate such scattering as continuous with a uniform anglular power density. This leads to the following definition.

Definition 3.5. *The fading is isotropic with respect to the mobile terminal if $\gamma(\theta) = 1/2\pi$ for all θ.*

For isotropic fading, (3.35) simplifies as

$$\begin{aligned} R_E(\xi) &= \frac{1}{2\pi} \int_{-\pi}^{\pi} e^{2\pi\nu_{\max}\xi\cos\theta} d\theta \\ &= \frac{1}{2\pi} \int_{-\pi}^{\pi} \cos(2\pi\nu_{\max}\xi\cos\theta) d\theta = J_0(2\pi\nu_{\max}\xi) \end{aligned} \tag{3.36}$$

where $J_0(\cdot)$ is the *zeroth order Bessel function of the first kind* [AS64].

$$\begin{aligned} J_0(x) &= \frac{1}{2\pi} \int_{-\pi}^{\pi} \cos(x\cos\theta) d\theta \\ &= \frac{1}{\pi} \int_0^{\pi} \cos(x\cos\theta) d\theta = \frac{2}{\pi} \int_0^{\pi/2} \cos(x\cos\theta) d\theta \, . \end{aligned} \tag{3.37}$$

Thus

Result 3.4. *For isotropic fading, $R_E(\xi)$ is real-valued:*

$$R_E(\xi) = 2R_{E_I}(\xi) = J_0(2\pi\nu_{max}\xi)\ . \tag{3.38}$$

and

$$R_{E_Q E_I}(\xi) = 0 \tag{3.39}$$

That is, the in-phase and quadrature processes are uncorrelated.

It is of interest to determine the accuracy of the Bessel ACF model for a "real" isotropic fading environment. To this end consider the scenario where there are N discrete paths that have angles that are uniformly distributed at the mobile terminal. In this case the $R_E(\xi)$ can be computed numerically using

$$R_E(\xi) = \frac{1}{N}\sum_{n=1}^{N} e^{j2\pi\nu_{\max}\xi\cos(2\pi/N)} \tag{3.40}$$

We see in Figure 3.6 that even for $N = 8, 16$ we get an ACF that is well approximated by a Bessel function.

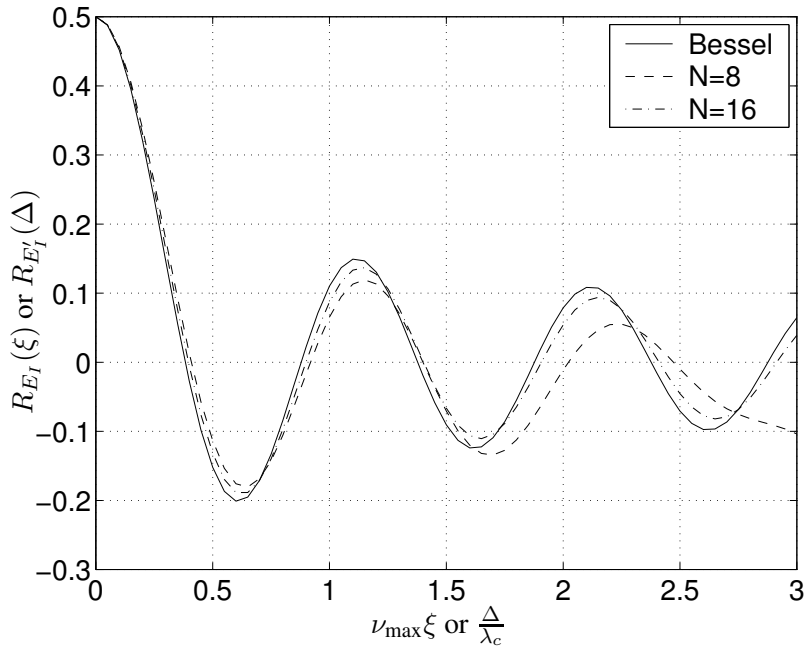

Figure 3.6: Accuracy of the Bessel approximation.

So far we have been able to characterize the mean and autocorrelation function of the flat fading process $E(t)$, using the key assumptions that the path phases are independent and uniformly distributed. Remarkably these assumptions give us the important properties that $E(t)$ is zero mean and proper. Our goal now is to make the statistical model for $E(t)$ more precise, but before we do that we distinguish between the cases where the multipath does or does not have a *specular* component. If the multipath is produced only from reflections from (rough) objects in the environment, then this form of scattering is said to be *purely diffuse* and can be approximated by a continuum of paths, with no one path dominating the others in strength. By

specular component is meant a subset of paths whose strengths significantly dominate the other paths. The most commonly encountered specular path is the line-of-sight (LOS) path, but specular paths may also be produced by smooth reflectors.

3.4.2 PURELY DIFFUSE SCATTERING - RAYLEIGH FADING

Now, if the number of paths is large and they are roughly of equal amplitudes, we may apply the Central Limit Theorem (see Result B.3) to conclude that $E(t)$ is a proper complex Gaussian (PCG) random process.

Thus, for purely diffuse scattering, we have the following:

Result 3.5. *$E(t)$ is well-modelled as a zero-mean, proper complex Gaussian process.*

First order statistics of $E(t)$ for purely diffuse scattering

For fixed t, $E(t) = E_I(t) + jE_Q(t)$ is a proper complex Gaussian random variable with

$$\mathsf{E}\left[|E(t)|^2\right] = \sum_n \beta_n^2 = 1\,. \tag{3.41}$$

Since $E(t)$ is proper, $E_I(t)$ and $E_Q(t)$ are uncorrelated and have the same variance, which equals half the variance of $E(t)$ (see (B.8)). Since $E(t)$ is also Gaussian, $E_I(t)$ and $E_Q(t)$ are independent as well. Thus

Result 3.6. *For fixed t, $E_I(t)$ and $E_Q(t)$ are independent $\mathcal{N}(0, 1/2)$ random variables.*

Definition 3.6. *The envelope process $\beta(t)$ and the phase process $\phi(t)$ are defined by*

$$\beta(t) = |E(t)| = \sqrt{E_I^2(t) + E_Q^2(t)}\,,$$

and

$$\phi(t) = \tan^{-1}\left(\frac{E_Q(t)}{E_I(t)}\right)\,.$$

We can write $y(t)$ of Figure 3.5 in terms of $\beta(t)$ and $\phi(t)$ as:

$$y(t) = g\beta(t)\, e^{j\phi(t)} s(t)\,. \tag{3.42}$$

This means that for flat fading, the channel is "seen" as a single path with gain $g\beta(t)$ and phase shift $\phi(t)$ that vary with time. Note that β and ϕ vary much more rapidly than the gains and phases of the individual paths β_n and ϕ_n. For fixed t, using the fact that $E_I(t)$ and $E_Q(t)$ are independent $\mathcal{N}(0, 1/2)$ random variables, it is easy to show that $\beta(t)$ and $\phi(t)$ are independent random variables with $\beta(t)$ having a Rayleigh pdf and $\phi(t)$ being uniform on $[0, 2\pi]$. The pdf of $\beta(t)$ is given by

$$p_\beta(x) = 2x\, e^{-x^2} u(x)\,. \tag{3.43}$$

It can be shown that

$$\mathsf{E}[\beta] = \sqrt{\pi/4}\,, \tag{3.44}$$

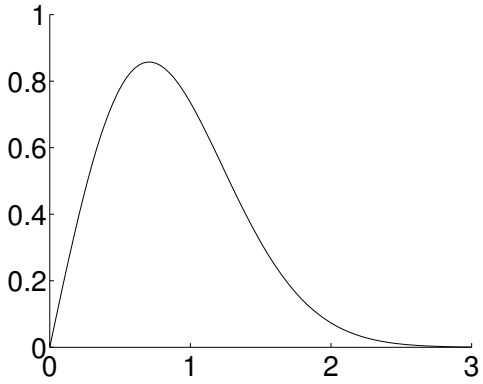

Figure 3.7: Rayleigh pdf

and that

$$\mathsf{E}[\beta^2] = \mathsf{E}\left[|E(t)|^2\right] = 1\,. \tag{3.45}$$

Note that if we scale the envelope β by the long-term gain g to produce $\beta' = \beta g$, then β' is also Rayleigh distributed with $\mathsf{E}[(\beta')^2] = g^2$, i.e.,

$$p_{\beta'}(x) = \frac{2x}{g^2}\exp\left(-\frac{x^2}{g^2}\right)u(x) \tag{3.46}$$

Since the envelope has a Rayleigh pdf, purely diffuse fading is referred to as *Rayleigh fading*. Since the process $E(t)$ is zero mean and Gaussian, its complete statistical characterization is captured in the autocorrelation function $R_E(t+\xi, t)$. Note that

Autocorrelation Function of Envelope and Squared-Envelope

The signal at the output of the flat fading channel is given by

$$y(t) = gE(t)s(t) = g\beta(t)\,e^{j\phi(t)}s(t)\,. \tag{3.47}$$

The channel introduces both phase and envelope fluctuations in the signal. However, envelope fluctuations directly affect the signal-to-noise ratio at the receiver, and are hence usually more important than phase fluctuations in determining communication system performance[1]. It is hence of interest to determine the autocorrelation function of the envelope fluctuations $\beta(t)$.

Since $\mathsf{E}[\beta(t)] = \sqrt{\pi/4}$ (see (3.44)), we have that the autocorrelation function $R_\beta(\xi)$ and the autocovariance function $C_\beta(\xi)$ are related as:

$$R_\beta(\xi) = C_\beta(\xi) + \frac{\pi}{4}\,. \tag{3.48}$$

The covariance function $C_\beta(\xi)$ can be computed exactly but its form is quite complicated and involves a hypergeometric function [Cla68]. A good approximation for $C_\beta(\xi)$ is [Stu96]:

$$C_\beta(\xi) \approx \frac{\pi}{16}|R_E(\xi)|^2\,. \tag{3.49}$$

[1]This is under the assumption that the channel variations can be tracked at the receiver.

The statistics of the squared-envelope process $\beta^2(t)$ are also of interest in applications since the instantaneous power (and SNR) at time t is proportional to $\beta^2(t)$. The first-order pdf of $\beta^2(t)$ is easily computed to be *exponential* as shown below:

$$p_{\beta^2}(x) = \frac{p_\beta(\sqrt{x})}{2\sqrt{x}} = e^{-x}u(x) \tag{3.50}$$

The auto-covariance function of $\beta^2(t)$ can be computed exactly, and it has a suprisingly simple form:

Result 3.7.

$$C_{\beta^2}(\xi) = |R_E(\xi)|^2 . \tag{3.51}$$

Proof. The proof follows easily from the fact for zero-mean, real-valued, jointly Gaussian random variables X_1, X_2, X_3 and X_4

$$\mathsf{E}[X_1X_2X_3X_4] = \mathsf{E}[X_1X_2]\mathsf{E}[X_3X_4] + \mathsf{E}[X_1X_3]\mathsf{E}[X_2X_4] + \mathsf{E}[X_1X_4]\mathsf{E}[X_2X_3]$$

■

Now since $\mathsf{E}[\beta^2(t)] = 1$, the auto-correlation function of $\beta^2(t)$ is given by

$$R_{\beta^2}(\xi) = 1 + C_{\beta^2}(\xi) = 1 + |R_E(\xi)|^2 . \tag{3.52}$$

We end our discussion of Rayleigh flat fading by plotting a typical sample path of a simulated Rayleigh fading envelope $|E(t)|$ in Figure 3.8. It can be seen that the fading can be quite severe with path losses of 10 to 20 dB over very small time scales. We will see in the next section that the fading is not as severe when there is a line of sight component in the scattering.

3.4.3 SCATTERING WITH A SPECULAR COMPONENT – RICEAN FADING

As mentioned earlier, when the scattering has a specular component, there may be more than one specular (dominant) path. We first consider the most commonly encountered scenario where there is only specular path, namely the line-of-sight (LOS) path. Without loss of generality, suppose that the LOS path is given the index of 1, with angle of arrival θ_1, gain β_1 and phase process

$$\phi_1(t) = \varphi_1 + 2\pi\nu_{\max}t\cos\theta_1 . \tag{3.53}$$

Then the flat fading process $E(t)$ of (3.13) gets modified as

$$E(t) = \beta_1\, e^{j\phi_1(t)} + \sum_{n=2}^{N} \beta_n\, e^{j\phi_n(t)} . \tag{3.54}$$

where gain of the LOS path β_1 is considerably larger than the gains of the diffuse components $\{\beta_n\}_{n=2}^N$. Now, since the small-scale variations are normalized to have a net average gain of 1, we have

$$\sum_{n=1}^{N} \beta_n^2 = 1 , \tag{3.55}$$

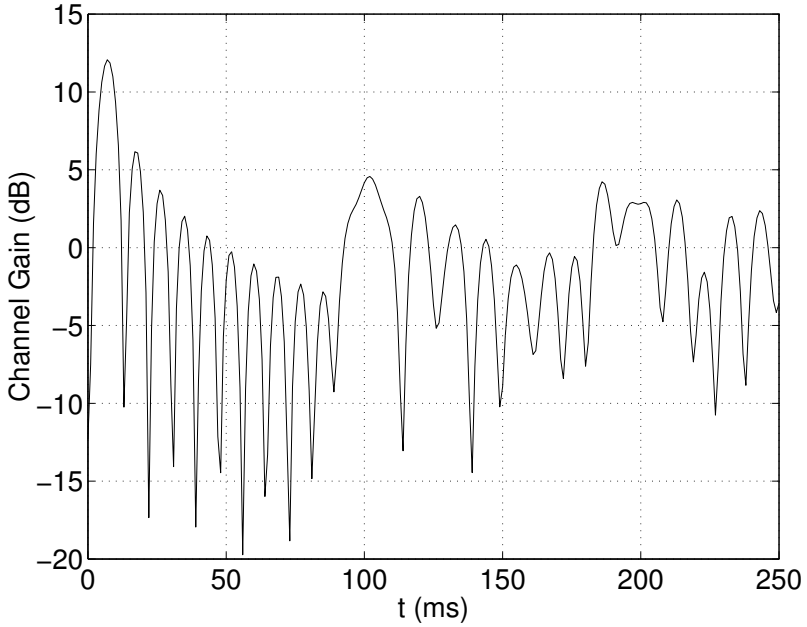

Figure 3.8: Rayleigh fading envelope for a carrier frequency of 900 MHz and mobile speed of 72 km/hr.

which implies that

$$\sum_{n=2}^{N} \beta_n^2 = 1 - \beta_1^2 \,. \tag{3.56}$$

This means we can write

$$\sum_{n=2}^{N} \beta_n \, e^{j\phi_n(t)} = \sqrt{1-\beta_1^2}\; \check{E}(t) \tag{3.57}$$

where $\check{E}(t)$ is a zero mean, proper complex Gaussian, Rayleigh fading process with variance $\mathsf{E}\left[|\check{E}(t)|^2\right] = 1$, i.e.,

$$R_{\check{E}}(\xi) = \int_{-\pi}^{\pi} \gamma(\theta) e^{j2\pi\nu_{\max}\xi\cos\theta} d\theta \,, \tag{3.58}$$

with $\gamma(\theta)$ being the angular gain density of the diffuse components.

Remark 3.1. *It is important to note that $E(t)$ is also a zero-mean process, but it cannot be modelled as Gaussian since the specular component $\beta_1 \, e^{j\phi_1(t)}$ dominates the diffuse components in power, and the Central Limit Theorem does not apply. However, conditioned on φ_1, $E(t)$ is indeed a proper complex Gaussian process with mean $\beta_1 \, e^{j\phi_1(t)}$.*

The relative strength of the specular component is captured in a quantity called the Rice factor defined as follows.

Definition 3.7. *The Rice factor κ is defined by*

$$\kappa = \frac{\textit{power in the specular component}}{\textit{total power in diffuse components}} = \frac{\beta_1^2}{1-\beta_1^2} \,. \tag{3.59}$$

From the definition of κ it follows that

$$\beta_1 = \sqrt{\frac{\kappa}{\kappa+1}}, \quad \text{and} \quad 1-\beta_1^2 = \frac{1}{(\kappa+1)}\,. \tag{3.60}$$

Thus we have

$$E(t) = \sqrt{\frac{\kappa}{\kappa+1}}\, e^{j\phi_1(t)} + \sqrt{\frac{1}{\kappa+1}}\, \check{E}(t)\,. \tag{3.61}$$

First Order Statistics of Ricean Fading

For fixed t, the pdf of the envelope $\beta(t)$ can be found by first computing the joint pdf of $\beta(t)$ and $\phi(t)$, conditioned on φ_1. This is facilitated by the fact that conditioned on φ_1, $E(t)$ is a proper complex Gaussian random variable with mean $\beta_1 e^{j\phi_1(t)}$. We then have:

Result 3.8. *The pdf of $\beta(t)$ conditioned on φ_1 is the Ricean pdf [Ric48], given by*

$$p_{\beta|\varphi_1}(x) = \frac{2x}{1-\beta_1^2}\, I_0\left(\frac{2x\beta_1}{1-\beta_1^2}\right)\, \exp\left[-\frac{x^2+\beta_1^2}{1-\beta_1^2}\right]\, u(x) \;=\; p_\beta(x) \tag{3.62}$$

where $I_0(\cdot)$ is the zeroth order modified Bessel function of 1st kind [AS64], i.e.,

$$I_0(y) = \frac{1}{2\pi}\int_{-\pi}^{\pi} \exp(y\cos\psi)d\psi\,. \tag{3.63}$$

Notice that the conditional pdf $p_{\beta|\varphi_1}(x)$ given in (3.62) is not a function of φ_1. This means that although $E(t)$ depends on φ_1, the evelope $\beta(t)$ is independent of φ_1. Thus the unconditional pdf of $\beta(t)$ is also given by the Ricean pdf of (3.62). The Ricean pdf can be rewritten in terms of κ as:

$$p_\beta(x) = 2x(\kappa+1)\, I_0\left(2x\sqrt{\kappa(\kappa+1)}\right)\, \exp\left[-x^2(\kappa+1)-\kappa\right]\, u(x)\,. \tag{3.64}$$

It is easy to see that when $\kappa = 0$, $p_\beta(x)$ of (3.64) reduces to a Rayleigh pdf (see (3.43)).

The pdf of $\beta^2(t)$ is also easily computed as:

$$p_{\beta^2}(x) = \frac{p_\beta(\sqrt{x})}{2\sqrt{x}} = (\kappa+1)\, I_0\left(2\sqrt{x\kappa(\kappa+1)}\right)\, \exp\left[-x(\kappa+1)-\kappa\right]\, u(x) \tag{3.65}$$

which reduces to the exponential pdf of (3.50) when $\kappa = 0$.

The presence of a LOS component makes the fading more benign, as in seen in Figure 3.10, where typical sample paths for Ricean envelopes with Rice factors of $\kappa = 5, 10$ are compared with Rayleigh fading.

Correlation and covariance functions for Ricean fading

From (3.61), exploiting the fact that the process $\phi_1(t)$ is independent of the process $\check{E}(t)$, it is easy to see that the autocorrelation function of $E(t)$ is given by:

$$\begin{aligned} R_E(\xi) &= \mathsf{E}\left[E(t+\xi)\; E^\star(t)\right] \\ &= \frac{\kappa}{\kappa+1}\, \mathsf{E}\left[\; e^{j[\phi_1(t+\xi)-\phi_1(t)]}\right] + \frac{1}{\kappa+1}\, R_{\check{E}}(\xi) \\ &= \frac{\kappa}{\kappa+1}\, e^{j2\pi\nu_{\max}\xi\cos\theta_1} + \frac{1}{\kappa+1}\, R_{\check{E}}(\xi) \end{aligned} \tag{3.66}$$

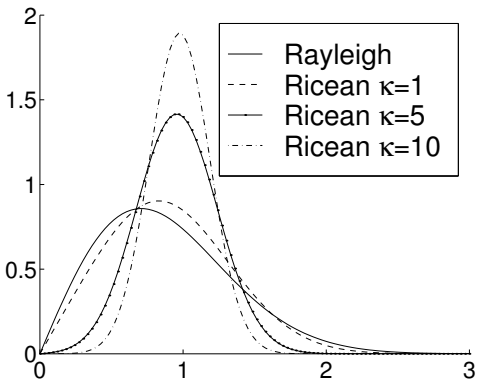

Figure 3.9: Ricean pdf for various Rice factors.

where $R_{\check{E}}(\xi)$ is given in (3.58). Note that the Ricean fading process is also stationary (over short time horizons corresponding to movements of the order of a few wavelengths in distance.)

For isotropic diffuse components (see (3.36)), we have

$$R_E(\xi) = \frac{\kappa}{\kappa+1}\, e^{j2\pi\nu_{\max}\xi\cos\theta_1} + \frac{1}{\kappa+1}\, J_0(2\pi\nu_{\max}\xi)\,. \tag{3.67}$$

Since $E(t)$ is proper, the auto- and cross-correlation functions of the inphase and quadrature processes $E_I(t)$ and $E_Q(t)$ are of course given in directly in terms of the real and imaginary parts of $R_E(\xi)$ (see (B.12)).

The covariance function $C_\beta(\xi)$ is not easy to compute for Ricean fading. However, $C_{\beta^2}(\xi)$ can be computed after some tedious but straightforward steps similar to those used in proving (3.51).

Result 3.9.

$$C_{\beta^2}(\xi) = \left(\frac{1}{\kappa+1}\right)^2 \left[|R_{\check{E}}(\xi)|^2 + 2\kappa \mathit{Re}\left[R_{\check{E}}(\xi)e^{j2\pi\nu_{max}\xi\cos\theta_1}\right]\right], \tag{3.68}$$

Note that (3.68)reduces to the covariance function for Rayleigh fading when $\kappa = 0$. However, for nonzero κ, $C_{\beta^2}(\xi) \neq |R_E(\xi)|^2$, but rather

$$C_{\beta^2}(\xi) = |R_E(\xi)|^2 + \left[\frac{\kappa}{\kappa+1}\right]^2. \tag{3.69}$$

Scattering With Multiple Specular Paths

If there is more than one specular path, we can rewrite (3.54) as

$$E(t) = \sum_{n=1}^{N_s} \beta_n\, e^{j\phi_n(t)} + \sum_{n=N_s+1}^{N} \beta_n\, e^{j\phi_n(t)} \tag{3.70}$$

where N_s is the number of specular paths.

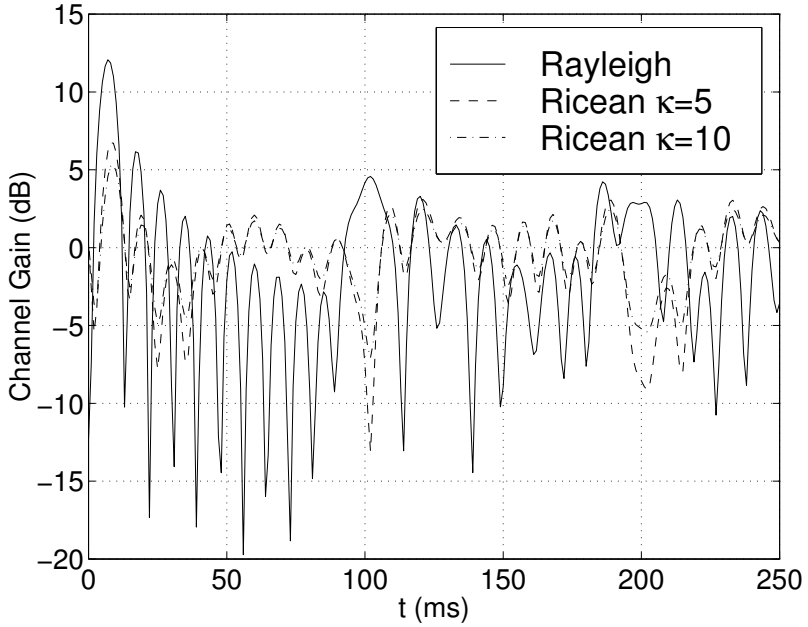

Figure 3.10: Ricean fading envelopes for a carrier frequency of 900 MHz and mobile speed of 72 km/hr.

A major difference between the case of one specular path and that with multiple specular paths is that the *unconditional* distribution of the envelope β is no longer Ricean. However, conditioned on the specular phases $\varphi_1, \ldots, \varphi_{N_s}$, the process $E(t)$ is proper complex Gaussian with mean $\sum_{n=1}^{N_s} \beta_n \, e^{j\phi_n(t)}$, and the envelope has a Ricean distribution with Rice factor

$$\kappa = \frac{\sum_{n=1}^{N_s} \beta_n^2}{\sum_{n=N_s+1}^{N} \beta_n^2} \tag{3.71}$$

Furthermore, the correlation and covariance functions described above for LOS Ricean fading get appropriately modified when there are multiple specular components.

3.4.4 FADING ACF AND COHERENCE DISTANCE/TIME

The fading model we have developed so far is for the (small scale) gain variations in time due to the mobile traveling with some velocity v. We can equivalently treat the gain variations as a random process in a distance variable ζ. Assuming that we are at distance ζ_0 from some reference point on the trajectory of the mobile at time $t = 0$, the distance at time t is given by

$$\zeta = \zeta_0 + vt \, . \tag{3.72}$$

We can define the fading process in the distance variable by

$$E'(\zeta) = E((\zeta - \zeta_0)/v) \tag{3.73}$$

and the corresponding auto-correlation function over the distance variable is given by

$$\begin{aligned} R_{E'}(\Delta) &= \mathsf{E}\left[E'(\zeta+\Delta)E'^{\star}(\zeta)\right] \\ &= R_E\left(\tfrac{\Delta}{v}\right) = R_E\left(\tfrac{\Delta}{\nu_{\max}\lambda_c}\right) \\ &= J_0\left(2\pi\tfrac{\Delta}{\lambda_c}\right) \quad \text{(for isotropic fading)} \end{aligned} \tag{3.74}$$

We now introduce the notion of coherence time (distance) which is a measure of how rapidly the channel varies.

Definition 3.8. *Coherence Distance. The coherence distance Δ_c is a measure how much the MS can move with $E'(\zeta)$ being roughly unchanged. We can define Δ_c more precisely in terms of the ACF as (say):*

$$\Delta_c = \textit{largest } \Delta \textit{ such that } |R_{E'}(\Delta)| > 0.9 R_{E'}(0) = 0.9$$

The justification for using the absolute value of $R_{E'}(\Delta)$ in the above definition is that the squared-envelope covariance function is a direct function of $|R_{E'}(\Delta)|^2$ (see (3.69)).

We can similarly define the coherence time T_c in terms of the ACF $R_E(\xi)$, but this is not necessary since we can define T_c in terms of Δ_c.

Definition 3.9. *Coherence Time. The coherence time is given by*

$$T_c = \frac{\Delta_c}{v} \, .$$

For isotropic Rayleigh fading, using (3.36), we can show that:

$$\Delta_c \approx 0.1\lambda_c \, , \text{ and } \; T_c \approx \frac{0.1}{\nu_{\max}} \, . \tag{3.75}$$

The coherence time of the channel naturally plays an important role in the estimation of the channel – the longer the coherence time, the easier it is to estimate the channel. For digital communications over fading channels, the relationship between the coherence time T_c and the symbol duration T_s is important in designing signaling strategies and in performance analysis. In this context, we have the following important definition.

Definition 3.10. *The fading process is said to be slow if*

$$T_c \gg T_s \, .$$

The slow fading assumption holds for most modern wireless communication systems. As an example, consider a system with $f_c = 1$ GHz, and suppose the maximum velocity $v_{\max} = 200$ km/hr ≈ 55 m/s. (It would be illegal for anyone to be on a terrestrial wireless terminal at speeds greater than this!) Then $f_m \approx 200$ Hz. If the symbol rate is greater than 1500 symbols/s (which is true for most applications of interest), then the fading is slow.

Angular spread of scattering and coherence distance/time

The ACF of $E(t)$ is a function of the angular spread (and angular location) of the propagation. If the support of the angular gain density $\gamma(\theta)$ is restricted to $\theta \in [\theta_1, \theta_2]$, then it follows from (3.27) that

$$R_{\check{E}}(\xi) = \int_{\theta_1}^{\theta_2} \gamma(\theta)\, e^{j2\pi\nu_{\max}\xi\cos\theta} d\theta\,. \tag{3.76}$$

In this case, $R_E(\xi)$ is not necessarily expressible in "closed-form", nor is it necessarily real-valued.

The isotropic scattering environment represents one extreme case for which the fading has the smallest coherence time. The other extreme case is when the angular spread is so small that the propagation is effectively on a single LOS path arriving at angle θ. In this case,

$$E(t) \approx \beta e^{-j(2\pi\nu_{\max} t\cos\theta + \phi)} \tag{3.77}$$

and the channel produces no envelope fluctuations in the signal, and simply shifts the frequency by $\nu_{\max}\cos\theta$ (assuming that the velocity is constant). This means that there is essentially no fading. Note, however, that it very unlikely that scattering would be diffuse when the angular spread is close to zero – this would only happen in the rare situation where the LOS path is blocked but only one other (diffuse) scatterer exists in the environment.

The absolute value of the ACF of $E(t)$ for Rayleigh fading is shown for various angular spreads in Figure 3.11. From this figure it is clear that $|R_E(\xi)|$, and hence Δ_c (or T_c), can be a strong function of the angular spread. For example in a environment with an angular spread of 30 degrees, the coherence time is 10 times larger than in an isotropic scattering environment. This dependence of correlation on angular spread will be even more significant in the context of frequency selective fading (see Section 3.5).

Finally, coherence times can be considerably larger for Ricean fading with the same angular spreads, as can be seen in Figure 3.12. This is because the LOS component "stabilizes" the channel considerably and makes the fading more benign.

3.4.5 POWER SPECTRAL DENSITY OF FREQUENCY FLAT FADING

For an arbitrary angular gain density $\gamma(\theta)$, it can be shown that the power spectral density (PSD) for the diffuse component of the flat fading process can be obtained in closed form by taking the Fourier transform of the auto-correlation function given in (3.58):

$$S_{\check{E}}(\nu) = \begin{cases} \dfrac{\gamma(\cos^{-1}(\nu/\nu_{\max})) + \gamma(-\cos^{-1}(\nu/\nu_{\max}))}{\sqrt{\nu_{\max}^2 - \nu^2}} & \text{for } |\nu| < \nu_{\max} \\ 0 & \text{otherwise} \end{cases} \tag{3.78}$$

The PSD of for a Ricean fading process with Rice factor κ and angle of arrival θ_1 for the LOS component is then given by the Fourier transform of the ACF given in (3.66):

$$S_E(\nu) = \frac{\kappa}{\kappa+1}\,\delta(\nu - \nu_{\max}\cos\theta_1) + \frac{1}{\kappa+1}\,S_{\check{E}}(\nu)\,. \tag{3.79}$$

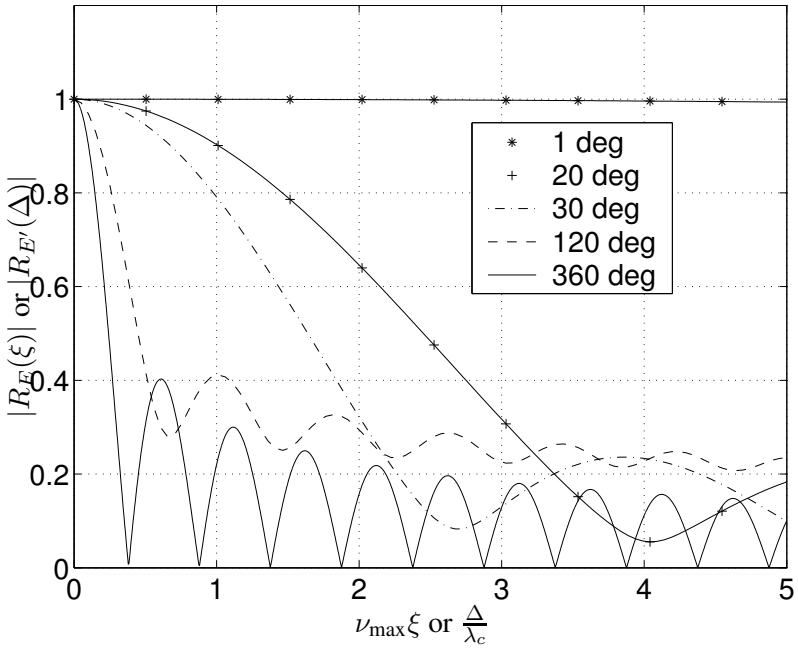

Figure 3.11: Correlation functions for various angular spreads around $\theta = 45$ deg for Rayleigh fading.

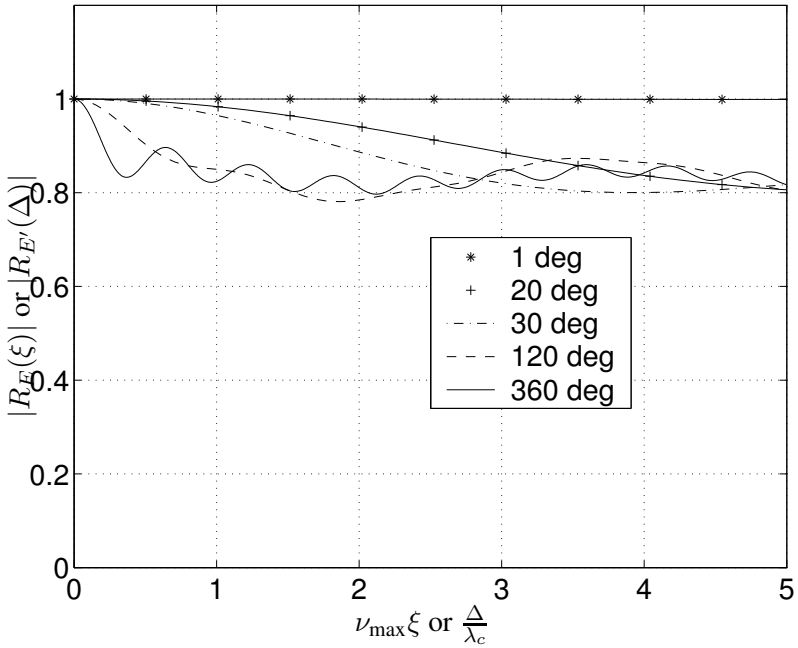

Figure 3.12: Correlation functions for various angular spreads around $\theta = 45$ deg for Ricean fading, with the LOS path at $\theta_0 = 45$ deg and Rice factor of $\kappa = 5$.

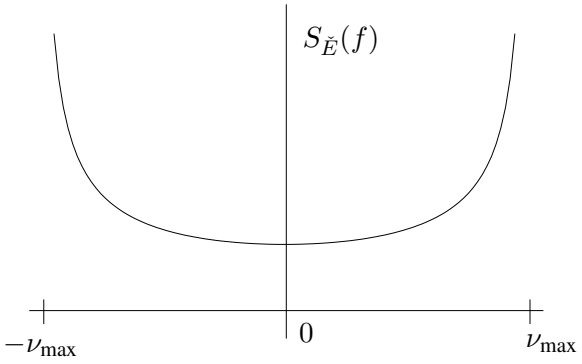

Figure 3.13: Power spectral density of isotropic flat fading.

For isotropic fading, the PSD of the diffuse components can be obtained from the Fourier transform of the Bessel function J_0 in the form given below.

$$S_{\check{E}_I}(\nu) = S_{\check{E}_Q}(\nu) = \frac{1}{2}\, S_{\check{E}}(\nu) = \begin{cases} \frac{1}{2\pi\sqrt{\nu_{\max}^2 - \nu^2}} & \text{if } |\nu| < \nu_{\max} \\ 0 & \text{otherwise} \end{cases}, \tag{3.80}$$

A plot of this PSD is shown in Figure 3.13.

If the transmitted passband signal is a pure carrier, i.e., $s(t) = 1$, and the fading is Rayleigh and isotropic, then from (3.31) we get that the PSD of the passband version $\tilde{y}(t)$ of $y(t)$ is

$$S_{\tilde{y}}(f) = \begin{cases} \frac{g^2}{2\pi\sqrt{\nu_{\max}^2 - (f - f_c)^2}} & \text{if } |f - f_c| < \nu_{\max} \\ \frac{g^2}{2\pi\sqrt{\nu_{\max}^2 - (f + f_c)^2}} & \text{if } |f + f_c| < \nu_{\max} \\ 0 & \text{otherwise} \end{cases}, \tag{3.81}$$

See page 75 of the book by Jakes [Jak74] for a plot of the ideal isotropic PSD and a comparison with simulations.

3.4.6 SIMULATION OF FREQUENCY FLAT FADING

Method 1: Direct Approach

① Pick the number of paths N.

② Pick the path gains, delays, and angles of arrival for a discrete set of paths corresponding to desired angular spread and angular location. For example, to simulate an isotropic Rayleigh fading environment, set $\beta_n = \sqrt{1/N}$, and $\theta_n = 2\pi n/N$, $n = 1, 2, \ldots, N$.

③ Approximate the path phase processes $\phi_n(t)$ by

$$\hat{\phi}_n(t) = \varphi_n - 2\pi\nu_{\max} t \cos\theta_n,$$

where φ_n are chosen to be i.i.d. Unif$[0, 2\pi]$.

④ Sum up paths, i.e., simulate $E(t)$ by

$$\hat{E}(t) = \sum_{n=1}^{N} \beta_n e^{j\hat{\phi}_n(t)} \, . \tag{3.82}$$

Method 2: Filtered White Gaussian Noise

① Find a discrete-time approximation to $E(t)$ by sampling, with sample period T_0, i.e.,

$$E[k] \approx E(kT_0) \, . \tag{3.83}$$

② Compute the corresponding discrete time autocorrelation function from the (known) continuous-time ACF $R_E(\xi)$ as

$$R_E[m] = \mathsf{E}\left[E[k+m]E^{\star}[k]\right] = R_E(mT_0) \, . \tag{3.84}$$

③ Find the "square-root" filter using spectral factorization [WH85]. That is, the filter $H(z)$ satisfies the

$$H(z)H(z^{-1}) = S_E(z) \, , \tag{3.85}$$

where $S_E(z)$ is the Z-transform of $R_E[m]$.

④ Pass a proper complex white Gaussian sequence, i.e., a sequence of $\mathcal{CN}(0,1)$ random variables, through the filter to produce samples of $E(t)$.

A Comment on Jakes' Simulation Method

Jakes [Jak74] suggested the following method to simulate isotropic Rayleigh *flat* fading (which is valid only for N such that $N/2$ is odd). He forms $E_I^{\mathrm{J}}(t)$ and $E_Q^{\mathrm{J}}(t)$ using the equations:

$$\begin{aligned} E_I^{\mathrm{J}}(t) &= \frac{2}{\sqrt{N}} \left[\cos\gamma \cos 2\pi\nu_{\max} t + \sqrt{2} \sum_{n=1}^{M} \cos\psi_n \cos 2\pi\nu_n t \right] , \\ E_Q^{\mathrm{J}}(t) &= \frac{2}{\sqrt{N}} \left[\sin\gamma \cos 2\pi\nu_{\max} t + \sqrt{2} \sum_{n=1}^{M} \sin\psi_n \cos 2\pi\nu_n t \right] , \end{aligned} \tag{3.86}$$

where $M = \frac{1}{2}(\frac{N}{2} - 1)$, $\nu_n = \nu_{\max} \cos(2\pi n/N)$, $\gamma = 0$ and $\psi_n = \pi n/M$.

The key point to be noted in the above equations is that an isotropic fading environment corresponding to N paths is being simulated using only about $N/4$ oscillators. The direct approach would need to have N terms in the sum for each of $\hat{E}_I(t)$ and $\hat{E}_Q(t)$. This implies a significant reduction in complexity if we are trying to simulate fading using hardware (which is what Jakes did!).

Jakes argues that the time correlation properties of the function $E^{\mathrm{J}}(t)$ generated by (3.86) approximate the ensemble correlation functions of an isotropic Rayleigh fading process. That is $E^{\mathrm{J}}(t)$ is a sample path of an isotropic Rayleigh fading process.

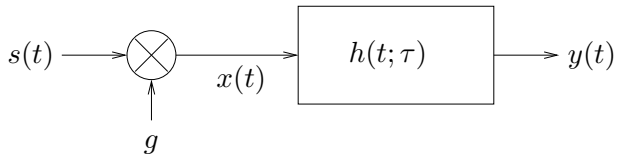

Figure 3.14: Channel model for general (possibly frequency selective) fading

If we denote the time average auto-correlation function of a random process $X(t)$ by $\hat{R}_X(t+\xi,t)$, then it is easy to show that

$$\begin{aligned}
\hat{R}_{E_I^{\mathrm{J}}}(\xi) &= \frac{2}{N}\left[\cos^2\gamma\cos(2\pi\nu_{\max}\xi) + 2\sum_{n=1}^{M}\cos^2\psi_n\cos(2\pi\nu_n\xi)\right] \\
\hat{R}_{E_Q^{\mathrm{J}}}(\xi) &= \frac{2}{N}\left[\sin^2\gamma\cos(2\pi\nu_{\max}\xi) + 2\sum_{n=1}^{M}\sin^2\psi_n\cos(2\pi\nu_n\xi)\right] \\
\hat{R}_{E_Q^{\mathrm{J}}E_I^{\mathrm{J}}}(\xi) &= \frac{2}{N}\left[\sin\gamma\cos\gamma\cos(2\pi\nu_{\max}\xi)\right. \\
&\qquad \left. +2\sum_{n=1}^{M}\sin\psi_n\cos\psi_n\cos(2\pi\nu_n\xi)\right] = \hat{R}_{E_I^{\mathrm{J}}E_Q^{\mathrm{J}}}(\xi)
\end{aligned} \tag{3.87}$$

Now if we plug in $\gamma = 0$ and $\psi_n = \pi n/M$ in the above equation, we can show that $\hat{R}_{E^J}(\xi)$ is a good approximation for $J_0(2\pi\nu_{\max}\xi)$ for large M.

However, the time correlation functions given in (3.87) are poor approximations to the ensemble correlation functions of an isotropic Rayleigh fading process for $\nu_{\max}\xi > 1$. Furthermore, the complex process that $E^{\mathrm{J}}(t)$ represents is not even proper (assuming ergodicity) since $\hat{R}_{E_I^{\mathrm{J}}}(\xi) \neq \hat{R}_{E_Q^{\mathrm{J}}}(\xi)$ and $\hat{R}_{E_Q^{\mathrm{J}}E_I^{\mathrm{J}}}(\xi) = \hat{R}_{E_I^{\mathrm{J}}E_Q^{\mathrm{J}}}(\xi)$.

In conclusion, there is really no sense in using Jakes' technique for simulating flat fading on a computer. The direct method described above produces much more accurate results and is much more general. A factor of 2 reduction in complexity can be obtained in the direct method if we wish to simulate an isotropic fading process.

3.5 FREQUENCY SELECTIVE FADING

We now revisit the channel model for small-scale variations under different assumptions than the ones we made in previous section. Recall that the passband signals $\tilde{s}(t)$ and $\tilde{x}(t)$ are assumed to have bandwidth of W, and hence $s(t)$ and $x(t)$ have (complex) baseband bandwidth of $W/2$. If $W \ll \frac{1}{\tau_{\mathrm{ds}}}$, then the fading is flat and we have the channel model that we studied in Section 3.4 with $h(t;\tau)$ being replaced by a multiplication by the flat fading process $E(t)$.

Table 3.1, taken from Paulraj and Papadias [PP97], shows the delay spreads for various environments. Most modern digital communications systems operate at bandwidths of greater than 100 KHz, which means that the flat fading model is rarely useful in practice.

Environment	Spread
Flat Rural	0.5 μs
Urban	5 μs
Hilly	20 μs
Mall	0.3 μs
Indoors	0.1 μs

Table 3.1: Typical delay spreads for various environments.

If $W > \frac{1}{\tau_{\text{ds}}}$, then the fading is said to be *frequency selective*, and $h(t;\tau)$ can no longer be replaced by a multiplication by the flat fading process $E(t)$ as in (3.12). The goal of this section is to study how the channel model should be modified to account for frequency selectivity.

3.5.1 PURELY DIFFUSE SCATTERING

As we did in the study of frequency flat fading, we first characterize the channel for the situation where the scattering is purely diffuse, i.e., there is no specular component. Recall that time-varying impulse response is given by

$$h(t;\tau) = \sum_n \beta_n e^{j\phi_n(t)}\ \delta(\tau - \tau_n) \tag{3.88}$$

where the phase process $\phi_n(t)$ evolves as:

$$\begin{aligned} \phi_n(t) &\approx \varphi_n + 2\pi\nu_n t \\ &= \varphi_n + 2\pi\nu_{\max} t\cos\theta_n \end{aligned} \tag{3.89}$$

with the phases $\{\varphi_n\}$ being i.i.d. Unif $[-\pi,\pi]$ (see Assumption 3.2 and (3.14)). We can rewrite (3.88) as

$$h(t;\tau) = \sum_n \beta_n e^{j\varphi_n}\ e^{j2\pi\nu_n t}\ \delta(\tau - \tau_n) \tag{3.90}$$

Before we develop a stochastic model for $h(t;\tau)$, we introduce two additional equivalent represensentations of the time-varying channel [Bel63].

Definition 3.11. *For a channel with impulse response $h(t;\tau)$, the time-varying transfer function is given by*

$$\begin{aligned} H(t;f) &= \int h(t;\tau)e^{-j2\pi f\tau}d\tau \\ &= \sum_n \beta_n e^{j\varphi_n}\ e^{j2\pi(\nu_n t - f\tau_n)} \end{aligned} \tag{3.91}$$

and the delay-Doppler spreading function is given by

$$\begin{aligned} C(\nu;\tau) &= \int h(t;\tau)e^{-j2\pi\nu t}dt\ . \\ &= \sum_n \beta_n e^{j\varphi_n}\ \delta(\nu - \nu_n)\ \delta(\tau - \tau_n) \end{aligned} \tag{3.92}$$

Statistical Characterization of $H(t;f)$

In characterizing the channel stochastically, it is easiest to deal with the time-varying transfer function $H(t;f)$ since it is written as a sum of complex exponentials (rather than impulses). Since H is a function of two variables, it must be modelled as a random *field*.

The contribution of the n-th path to $H(t,f)$ can be written as

$$\eta_n(t;f) = \beta_n e^{j\varphi_n}\ e^{j2\pi(\nu_n t - f\tau_n)} \tag{3.93}$$

Analogous to the result we derived earlier in the context of frequency flat fading (Result 3.2), $\eta_n(t;f)$ can easily be seen to be a zero-mean proper complex field. Now the Central Limit Theorem (Result B.3) can be applied to obtain:

Result 3.10. *For purely diffuse scattering, $H(t;f)$ is well-modelled as a zero-mean, proper complex Gaussian random field.*

As a consequence, for fixed t, f, the magnitude $|H(t;f)|$ has a Rayleigh distribution and the phase $\angle H(t;f)$ is uniformly distributed on $[-\pi,\pi]$.

With the zero-mean proper complex Gaussian model for $H(t;f)$, all that is needed to completely characterize it stochastically is the autocorrelation function. Mimicking the derivation in (3.20), we have

$$\mathsf{E}\left[H(t_1;f_1)H^\star(t_2;f_2)\right] \approx \sum_n \beta_n^2\ e^{j2\pi\nu_n(t_1-t_2)}\ e^{-j2\pi\tau_n(f_1-f_2)}\ . \tag{3.94}$$

Thus $H(t;f)$ is approximately stationary in both t and f, i.e., it is approximately a *homogeneous* random field. The homogeneous autocorrelation function can then be defined as

$$\begin{aligned} R_H(\xi;\zeta) &= \mathsf{E}\left[H(t+\xi;f+\zeta)H^\star(t;f)\right] \\ &\approx \sum_n \beta_n^2\ e^{j2\pi\nu_n\xi}\ e^{-j2\pi\tau_n\zeta}\ . \end{aligned} \tag{3.95}$$

Using the fact that $\nu_n = \nu_{\max}\cos\theta_n$, we can rewrite (3.95) as

$$R_H(\xi;\zeta) = \sum_n \beta_n^2\ e^{j2\pi\nu_{\max}\xi\cos\theta_n}\ e^{-j2\pi\tau_n\zeta} \tag{3.96}$$

As in (3.35), we can express the autocorrelation function $R_H(\xi;\zeta)$ in terms of a power gain density. To this end, we generalize the angular gain density $\gamma(\theta)$ to a joint density that describes the allocation of power to both angle of arrival and delay.

Definition 3.12. *The joint angle-delay gain density $\gamma(\theta;\tau)$ is given by*

$$\gamma(\theta;\tau) = \sum_n \beta_n^2\ \delta(\theta-\theta_n)\ \delta(\tau-\tau_n)\ . \tag{3.97}$$

The discrete joint density of (3.97) can be approximated by continuous density, by considering the paths to be forming a *continuum*. As mentioned earlier, the continuous model is representative of diffuse scattering. Furthermore, the angular gain density $\gamma(\theta)$ is the marginal of $\gamma(\theta;\tau)$, i.e.,

$$\gamma(\theta) = \int_0^{\tau_{\text{ds}}} \gamma(\theta;\tau)d\tau\ . \tag{3.98}$$

Based on (3.97), we can rewrite (3.96) as

$$R_H(\xi;\zeta) = \int_{-\pi}^{\pi}\int_{0}^{\tau_{\text{ds}}} \gamma(\theta;\tau)\; e^{j2\pi\nu_{\max}\xi\cos\theta}\; e^{-j2\pi\tau\zeta}\; d\tau d\theta \tag{3.99}$$

GWSSUS Model and Scattering Function

The zero-mean proper complex Gaussian field model for $H(t;f)$ implies that the time-varying transfer function, $h(t;\tau)$, and the delay-Doppler spreading function, $C(\nu;\tau)$, are both also zero-mean proper complex Gaussian fields.

The autocorrelation function of $h(t;\tau)$ is easily shown to be

$$\mathsf{E}\left[h(t_1;\tau_1)h^{\star}(t_2;\tau_2)\right] = \left[\sum_n \beta_n^2\; e^{j2\pi\nu_n(t_1-t_2)}\; \delta(\tau_1-\tau_n)\right]\; \delta(\tau_1-\tau_2) \tag{3.100}$$

Note that $h(t;\tau)$ is not a homogeneous random field since it is not stationary in the delay variable τ. However, it is indeed stationary in the time variable and *uncorrelated* in the delay variable. The continuous path generalization of this model for $h(t;\tau)$ is referred to as the Gaussian Wide Sense Stationary Uncorrelated Scattering (GWSSUS) model, and was first studied in great detail by Bello [Bel63]. For the continuous path generalization, we can rewrite autocorrelation function in terms of the angle-Delay gain density as

$$\mathsf{E}\left[h(t+\xi;\tau_1)h^{\star}(t;\tau_2)\right] = \left[\int_{-\pi}^{\pi}\int_{0}^{\tau_{\text{ds}}} \gamma(\theta;\tau)\; e^{j2\pi\nu_{\max}\xi\cos\theta}\; \delta(\tau_1-\tau)\; d\tau d\theta\right] \delta(\tau_1-\tau_2) \tag{3.101}$$

The autocorrelation function of the delay-Doppler spreading function, $C(\nu;\tau)$, is given by

$$\mathsf{E}\left[C(\nu_1;\tau_1)C^{\star}(\nu_2;\tau_2)\right] = \left[\sum_n \beta_n^2\; \delta(\nu_1-\nu_n)\; \delta(\tau_1-\tau_n)\right]\; \delta(\tau_1-\tau_2)\; \delta(\nu_1-\nu_2)\,. \tag{3.102}$$

Thus, $C(\nu;\tau)$ is not stationary in ν or τ, but it is uncorrelated in both variables. It is interesting to see to that the quantity inside the square brackets on the RHS of (3.102) describes the distribution of power as a function of the Doppler frequency and delay. This leads to the following definition.

Definition 3.13. *The delay-Doppler scattering function is given by*

$$\Psi(\nu;\tau) = \sum_n \beta_n^2\; \delta(\nu-\nu_n)\; \delta(\tau-\tau_n)\,. \tag{3.103}$$

Thus

$$\mathsf{E}\left[C(\nu_1;\tau_1)C^{\star}(\nu_2;\tau_2)\right] = \Psi(\nu_1;\tau_1)\; \delta(\tau_1-\tau_2)\; \delta(\nu_1-\nu_2)\,. \tag{3.104}$$

The scattering function can approximated by a continuous (smooth) function for purely diffuse scattering. The support of the scattering function is restricted to the rectangular region $[-\nu_{\max},\nu_{\max}]\times[0,\tau_{\text{ds}}]$.

Obviously, there is a one-one relationship between the scattering function, $\Psi(\nu;\tau)$, and the angle-delay gain density $\gamma(\theta,\tau)$. A straightforward change of variables argument yields

$$\gamma(\theta,\tau) = \nu_{\max}\sin\theta\; \Psi(\nu_{\max}\cos\theta,\tau)\,. \tag{3.105}$$

3.5.2 SCATTERING WITH AN SPECULAR COMPONENT

If there is a specular component (with possibly multiple paths) in addition to the diffuse paths, then we can write the time-varying transfer function as

$$H(t;f) = \sum_{n=1}^{N_s} \beta_n \, e^{j\varphi_n} \, e^{j2\pi(\nu_n t - \tau_n f)} + \tilde{\beta} \, \check{H}(t;f) \tag{3.106}$$

where $\check{H}(t;f)$ is a zero-mean, proper complex Gaussian, homogeneous field of the kind described in the previous section, and

$$\tilde{\beta}^2 = 1 - \sum_{n=N_s+1}^{N} \beta_n^2 \, . \tag{3.107}$$

Thus, $H(t;f)$ is a zero-mean, proper complex, homogeneous field, but is non-Gaussian. However, conditioned on $\varphi_1, \ldots, \varphi_{N_s}$, $H(t;f)$ is a proper complex, non-homogeneous field, with non-zero mean. Also, just as in the case of the flat fading process $E(t)$, for fixed t, f, the distribution of the envelope $|H(t;f)|$, conditioned on $\varphi_1, \ldots, \varphi_{N_s}$, is Ricean with Rice factor given in (3.71). If there is only one specular path, the unconditional distribution of $|H(t;f)|$ is also Ricean.

The time-varying impulse response and delay-Doppler spreading functions get modified in a similar fashion:

$$h(t;\tau) = \sum_{n=1}^{N_s} \beta_n \, e^{j\varphi_n} \, e^{j2\pi\nu_n t} \delta(\tau - \tau_n) + \tilde{\beta} \, \check{h}(t;\tau) \tag{3.108}$$

where $\check{h}(t;\tau)$ is a zero-mean, GWSSUS field.

$$C(\nu;\tau) = \sum_{n=1}^{N_s} \beta_n \, e^{j\varphi_n} \, \delta(\nu - \nu_n) \, \delta(\tau - \tau_n) + \tilde{\beta} \, \check{C}(\nu;\tau) \tag{3.109}$$

where $\check{C}(\nu;\tau)$ is a zero-mean Gaussian field that is uncorrelated in ν and τ.

The autocorrelation functions of $H(t;f)$, $h(t;\tau)$, and $C(\nu;\tau)$ can be derived as straightforward extensions to those obtained previously for purely diffuse scattering.

Appendix C

Random Fields

Definition C.1. *A random field $V(x, y)$ is said to be homogeneous (or stationary) if for all n, and all choices of $(x_1, y_1), \ldots, (x_n, y_n)$, and (v_x, v_y), the joint distribution of $V(x_1, y_1), \ldots, V(x_n, y_n)$ is the same as that of $V(x_1 + v_x, y_1 + v_y), \ldots, V(x_n + v_x, y_n + v_y)$. That is, the joint distribution is invariant to translations.*

Note that for a homogeneous field, the joint distribution between the field at two points (say $V(x_1, y_1)$ and $V(x_2, y_2)$) is a function only of the vector joining them, i.e. $(x_2 - x_1, y_2 - y_1)$.

Definition C.2. *A random field $V(x, y)$ is said to be homogeneous and isotropic if for all n, and all choices of $(x_1, y_1), \ldots, (x_n, y_n)$, the joint distribution of $V(x_1, y_1), \ldots, V(x_n, y_n)$ is the same as that of $V(\mathcal{T}_1(x_1, y_1)), \ldots, V(\mathcal{T}_n(x_n, y_n))$, where*

$$\mathcal{T}((x_1, y_1), \ldots, (x_n, y_n)) = (\mathcal{T}_1(x_1, y_1), \ldots, \mathcal{T}_n(x_n, y_n))$$

is any transformation on the points $(x_1, y_1), \ldots, (x_n, y_n)$ that preserves distances between any pair of these points. That is, the joint distribution is invariant to rigid-body motions, i.e., translation followed by rotation (see Figure C.1).

For a homogeneous and isotropic random field, the joint distribution between the field at two points (say $V(x_1, y_1)$ and $V(x_2, y_2)$) is a function only of the distance Δ between them. That is

$$\mathsf{E}[V(x_1, y_1)\, V(x_2, y_2)] = R_V(\Delta), \quad \text{where } \Delta = \sqrt{(x_2 - x_1)^2 + (y_2 - y_1)^2}. \tag{C.1}$$

Bibliography

[Cla68] Clarke R. (July-August 1968) A statistical theory of mobile radio reception. *Bell Syst. Tech. J.* 47(6): 957–1000.

[Gud91] Gudmundson M. (1991) Correlation model for shadow fading in mobile radio systems. *Electron. Lett.* 27(23): 2145–2146.

[HJ85] Horn R. A. and Johnson C. R. (1985) *Matrix Analysis*. Cambridge, New York.

[AS64] Abramowitz M. and Stegun I. A. (1964) *Handbook of Mathematical Functions*. Dover, New York.

[NM93] Neeser F. D. and Massey J. L. (July 1993) Proper complex random processes with applications to information theory. *IEEE Trans. Inform. Th.* 39(4).

[Par98] Parsons J. D. (1998) *The Mobile Radio Propagation Channel*. Wiley, Chichester, England.

[PP97] Paulraj A. J. and Papadias C. B. (November 1997) Space-time processing for wireless communications. *IEEE Signal Processing Magazine* pages 49–83.

[Bel63] P. A. Bello. Characterization of randomly time-variant linear channels. *IEEE Trans. Commun. Systems*, pages 360–393, December 1963.

[Pro95] Proakis J. G. (1995) *Digital Communications*. Mc-Graw Hill, New York, 3rd edition.

[Rap96] Rappaport T. S. (1996) *Wireless Communications: Principles and Practice*. Prentice Hall, Upper Saddle River, NJ.

[Ric48] Rice S. (January 1948) Statistical properties of a sine wave plus noise. *Bell Syst. Tech. J.* 27(1): 109–157.

[Stu96] Stuber G. (1996) *Principles of Mobile Communication*. Kluwer Academic, Norwell, MA.

[Jak74] Jakes, W. C., Jr. (1974) *Microwave Mobile Communications*. Wiley, New York.

[WH85] Wong E. and Hajek B. (1985) *Stochastic Processes in Engineering Systems*. Springer-Verlag, New York.

[Kai59] Kailath T. (May 1959) Sampling models for linear time-variant filters. Tech. Rep. 352, MIT Research Laboratory of Electronics.

[Koz97] Kozek W. (Jan. 1997) On the transfer function calculus for underspread LTV channels. *IEEE Trans. Signal Processing* pages 219–223.

[SA99] Sayeed A. M. and Aazhang B. (Jan. 1999) Joint multipath-Doppler diversity in mobile wireless communications. *IEEE Trans. Commun.* 47(1): 123–132.

[Sle76] Slepian D. (Mar. 1976) On bandwidth. *Proc. IEEE* 64(3): 292–300.

[AOS98] Asztély D., Ottersten B., and Swindlehurst A. L. (Feb. 1998) Generalised array manifold model for wireless commuinication channels with local scattering. *IEE Proc. Radar, Sonar Navig.* 145(1): 51–57.

[Bre78] Brewer J. W. (Sep. 1978) Kronecker products and matrix calculus in system theory. *IEEE Trans. Circ. and Syst.* 25(9): 772–781.

[FMB98] Fuhl J., Molisch A. F., and Bonek E. (Feb. 1998) Unified channel model for mobile radio systems with smart antennas. In *IEE Proc. Radar, Sonar Navig.*, volume 145, pages 32–41.

[Fos96] Foschini G. J. (1996) Layered space-time architecture for wireless communication in a fading environment when using multi-element antennas. *Bell Labs Tech. J.* 1(2): 41–59.

[GBGP00] Gesbert D., Bölcskei H., Gore D. A., and Paulraj A. J. (July 2000) Outdoor MIMO wireless channels: Models and performance prediction. *submitted to the IEEE Trans. Commun.* .

[Jak74] Jakes W. C. (1974) Mobile radio propagation. In Jakes W. C. (ed) *Microwave Mobile Communications*, pages 11–78. Wiley.

[JD93] Johnson D. H. and Dudgeon D. E. (1993) *Array Signal Processing*. Prentice Hall.

[LZM01] Luo J., Zeidler J. R., and McLaughlin S. (Jan. 2001) Performance analysis of compact antenna arrays with MRC in correlated nakagami fading channels. *IEEE Trans. Vehic. Tech.* 50(1): 267–277.

[OSW94] Ozarow L. H., Shamai S., and Wyner A. D. (1994) Information theoretic considerations for cellular mobile radio. *IEEE Trans. Vehic. Tech.* VT-43: 359–378.

[PP97] Paulraj A. J. and Papadias C. B. (Nov. 1997) Space-time processing for wireless communications. *IEEE Signal Processing Magazine* pages 49–83.

[RC98] Raleigh G. G. and Cioffi J. M. (Mar. 1998) Spatio-temporal coding for wireless communication. *IEEE Trans. Commun.* pages 357–366.

[SFGK00] Shiu D., Foschini G., Gans M., and Kahn J. (Mar. 2000) Fading correlation and its effect on the capacity of multielement antenna systems. *IEEE Trans. Commun.* pages 502–513.

[SR01] Svantesson T. and Ranheim A. (May 2001) Mutual coupling effects on the capacity of multielement antenna systems. In *Proc. ICASSP 01*.

[SW86] Stark H. and Woods J. W. (1986) *Probability, Random Processes, and Estimation Theory for Engineers*. Prentice Hall, New Jersey.

[Tel95] Telatar E. (June 1995) Capacity of multi-antenna gaussian channels. *AT& T-Bell Labs Internal Tech. Memo.* .

[TSC98] Tarokh V., Seshadri N., and Calderbank A. R. (Mar. 1998) Space-time codes for high data rate wireless communication: Performance criteria and code construction. *IEEE Trans. Inform. Th.* pages 744–765.

[VP01] Vian J. and Popović Z. (June 2001) Smart lens antenna arrays. In *IEEE 2001 International Microwave Symposium*. Phoenix.

